#3

TRAVELING DENSITY VARIATIONS IN PARTIALLY IONIZED GASES

ROBERT SHANKLIN COOPER

TECHNICAL REPORT 424

SEPTEMBER 2, 1964

MASSACHUSETTS INSTITUTE OF TECHNOLOGY
RESEARCH LABORATORY OF ELECTRONICS
CAMBRIDGE, MASSACHUSETTS

The Research Laboratory of Electronics is an interdepartmental laboratory in which faculty members and graduate students from numerous academic departments conduct research.

The research reported in this document was made possible in part by support extended the Massachusetts Institute of Technology, Research Laboratory of Electronics, jointly by the U.S. Army (Electronics Materiel Agency), the U.S. Navy (Office of Naval Research), and the U.S. Air Force (Office of Scientific Research) under Contract DA36-039-AMC-03200(E); and in part by Grant DA-SIG-36-039-61-G14; additional support was received from the National Science Foundation (Grant G-24073).

MASSACHUSETTS INSTITUTE OF TECHNOLOGY

RESEARCH LABORATORY OF ELECTRONICS

Technical Report 424

September 2, 1964

TRAVELING DENSITY VARIATIONS IN PARTIALLY IONIZED GASES

Robert Shanklin Cooper

Submitted to the Department of Electrical Engineering, M.I.T., September 6, 1963, in partial fulfillment of the requirements for the degree of Doctor of Science.

(Manuscript received February 10, 1964)

Abstract

This report deals with the problem of the propagation of macroscopic waves of ionization within the positive column of glow discharge tubes. In the literature of this field these waves have been called "moving striations" because of the visible radiation emanating from the traveling pulse. Both experimental and theoretical analyses of this phenomenon have been made. The principal experimental result of this work is the establishment of a linear regime of operation for the observed traveling waves and the artificial excitation of them. The principal theoretical result is the derivation and the analysis of a linear theory that is applicable to the experimental regime of operation.

TABLE OF CONTENTS

CONTENTS

I. INTRODUCTION

1.1 DESCRIPTION OF THE PROBLEM

The theory describing the plasma generated in a direct-current glow discharge was first outlined by Schottky,[1] in 1924. A further description of the plasma in the positive column of DC discharges, as well as a discussion of the physics governing the operation of the device as a whole, was published by von Engel and Steenbeck[2] somewhat later. Since these initial descriptions, the steady-state operation of direct-current electrical discharges in gases has been exhaustively treated by many workers. As a result, the steady-state behavior is rather well understood.

One problem that still remains is the unsteady behavior exhibited by glow discharges over a wide range of operating conditions for which the operation should be steady according to the classical theories. This behavior is characterized by oscillations in the terminal voltage and current of the discharge which are quite independent of the external circuit. Under some circumstances these oscillations are relatively smooth, periodic functions of time. Furthermore, it has been discovered that disturbances exist within the plasma during the oscillations which are periodic in both space and time and travel through the plasma at great rates of speed.

These disturbances usually occur in discharge tubes operated in the range of gas pressures above 1 mm Hg. They are accompanied by periodic, moving variations in the light intensity of the positive column; but they are usually undetectable by the human eye because of their high velocity. Frequencies of occurrence range from hundreds of cycles per second to hundreds of kilocycles.

The specific unsteady behavior of the plasma which results in moving density disturbances in the positive column of DC discharge tubes will be the central consideration of this report.

1.2 HISTORICAL DEVELOPMENT

In 1925, in the British journal Engineering, the following report was published[3]:

> "In three Tyndall Lectures recently given at the Royal Institution, Professor R. Whiddington, of Leeds, demonstrated, with the aid of modern resources and from modern points of view, both familiar and novel vacuum discharge phenomena which have not lost their charm since 1858, when they were first studied by Plucker and Geissler, by Tyndall, Warren de la Rue and others, but which still await their ultimate explanation."

One of the topics that Professor Whiddington's lectures touched upon was that of the "moving flashes" he had observed with rotating mirrors in the persistent spark discharges then being used by spectroscopists. After nearly forty years of exposure to physical inquiry, the phenomenon of the "moving flashes" still awaits an "ultimate explanation."

Whiddington's extensive observations, in 1925, of the phenomenon now called "moving striations" were not the first. Indeed, a German physicist named Wullner had observed

them, in 1874, using the same technique that had been used more than fifty years earlier. Following that, Spottiswood,[5] having read of Wullner's investigations, made extensive observations of his own, in 1876. Although Wullner had confined his experiments to discharges in hydrogen, Spottiswood tried many different kinds of gases and vapors. All exhibited the strange effect in one form or another.

In the period 1876-1925 there were few published accounts of investigations of moving striations. A notable exception to this, however, was a study by Aston[6] and Kikuchi, in 1920, in helium and neon capillary tubes, and a separate effort by Kikuchi,[7] in 1921.

There were probably two reasons for the relative inactivity indicated by the lack of published results during this period. First, the only method for observing these phenomena which was available to researchers of that period was the rotating mirror; and there was apparently not much new information to be gleaned by using that device. Second, the attention of many investigators[8, 9] was focused on the standing striations that had been observed in electrical discharges from the earliest times. Many thought, as some still do, that as soon as the standing striations were understood then moving striations would be easily explainable.

In the decade following 1925 there were numerous scientific publications dealing with the problem of moving striations. Several events contributed to this sudden surge of interest. Foremost among these was the development by Langmuir[10] of the theory of electron and ion plasma oscillations, which stimulated a vigorous interest in the unsteady behavior of supposedly quiescent discharges. Next in importance was the development, also by Langmuir,[11] of a rational theory of small probing electrodes by which the operational behavior of electrical discharges in gases could be meaningfully interpreted. Finally, the use of more sophisticated electronic instrumentation, such as vacuum tubes and cathode-ray oscilloscopes, in the analysis of the laboratory behavior of DC discharges was just becoming widespread.

Important contributions during the period were those of Fox,[12] Sloane and Minnis,[13] and Pupp.[14] Fox used radiofrequency receiving and amplifying equipment to "listen" to the unsteady discharges. Sloane and Minnis used time-resolved spectroscopy in an attempt to clarify the processes involved in the motion of the wave of ionization and excitation comprising the moving striations. Pupp was the first person to use probes and an oscilloscope to analyze a tube with moving striations.

During the Second World War and the years just preceding and following it, only isolated experimental work was done in an attempt to understand moving striations. In 1951, however, Donahue and Dieke,[15] working at Johns Hopkins University, made an exhaustive study of the motion of moving striations in many different types of tubes and gases. They principally examined light that was being emitted from them with phototubes and a cathode-ray oscilloscope; but they limited their comments concerning the explanation of the observed effects to a minor bit of speculation about metastable levels and delayed ionization.

Since the experiments performed by Donahue and Dieke, there has been a veritable

deluge of publications concerning this problem. Among the best papers in recent years have been those of Stewart,[16, 17] a student of Donahue and Dieke. Unfortunately, the number of observations and the diversity of viewpoints have not always served to increase the knowledge and decrease the confusion in this area. Indeed, much contradictory testimony is available even from distinguished investigators. All of them, however, have recognized and attested to the complexity of the problem.

Various experimental techniques have been used to examine DC discharge tubes exhibiting moving striations. Chronologically, they appeared in the following order:

1. rotating mirrors and rotating camera photography,
2. radio receivers attached to external capacitive probes,
3. Langmuir probes combined with cathode-ray oscilloscopes,
4. time-resolved spectroscopy,
5. phototubes combined with cathode-ray oscilloscopes, and
6. microwave diagnostics.

Thomson[8] used probing electron beams on standing striations, but the relatively high pressures at which moving striations occur precluded the use of beams for probing moving striations.

The history of the theoretical work done on this problem is not nearly so extensive. Four people have published theories that were deliberate attempts to solve the problem. They are Druyvesteyn,[18] Pekarek,[19] Robertson,[20] and Stewart.[17] The first two efforts are phenomenological theories, the one by Druyvesteyn being proposed in 1934. The last two are more oriented toward the microphysical asepcts of the problem. The main points of these theories will be discussed in this report, even though none has been noted for its success.

Several other authors have hinted that their solutions to the general problem of "plasma oscillations" have generated the solution to the problem of moving striations as a by-product of that work.[21, 22] Close scrutiny of these claims always proves them to be somewhat optimistic.

Although the literature dealing with moving striations is extensive and often confusing, certain general conclusions can be drawn from it and should be stated. First, it is clear that the plasma existing in direct-current discharge tubes, under conditions that can in no way be interpreted as extreme, can be spontaneously and irrefutably unstable. Second, the oscillations, resulting from this instability, which are virtually independent of the external circuitry, are important because they cause variations in the terminal voltage and current of the device that are sometimes in excess of 10 per cent of their average values. Third, the number and diversity of the published observations, both intentional and casual, prove beyond reasonable doubt that the existence of these waves is a fundamental and universally occurring phenomenon in this type of discharge. If they are dependent upon some one specific property of the device or of the included discharge medium, then it is a property universally shared by all. Fourth, the number of conflicting reports of the properties of moving striations raises the possibility that

more than one phenomenon is involved. Hence, different investigators may in fact be viewing entirely different phnomena. Fifth, it is clear that the basic physical processes that are acting to produce the observed phenomena have not been conclusively revealed by any of the published experiments or theories.

As is evidenced by the history of this problem, which covers a period of ninety years, it is an important one, if only in terms of the human effort already invested in its solution. It is certainly important in its own right, too. The DC discharge was probably the first device used to produce a plasma in the laboratory. Yet, properties of the device as fundamental as its stability and its spontaneous oscillation are not understood today. Any contribution to this understanding is a contribution to the basic understanding of plasma physics.

1.3 OBJECTIVES OF THE PRESENT RESEARCH

The objectives of this research were twofold. First, a comprehensive study of the detailed physical nature of spontaneously occurring moving striations was to be carried out. Second, a rational theory, based on the principal findings of the physical study, was to be constructed. The former objective was achieved through a three-part program of literature search, laboratory experimentation, and theoretical analysis of the operating condtions of DC discharges. The latter objective was modified by the discovery during the experimentation that a quasi-linear regime of operation exists under certain conditions. This fact allows one to make a linear analysis of the problem and leads to an important result concerning the underlying cause of the plasma instability.

The organization of this research follows closely the chronological development of the work toward the main objectives. In Section II the details of laboratory observations of moving striations are considered at some length. Langmuir's ion sound-wave theory is considered and shown to be inapplicable. The results of detailed Langmuir-probe studies of spontaneous moving striations are given and analyzed. Conclusions are drawn concerning the important processes at work in the positive column during the wave motion.

Section III describes the experiments mentioned above in which initially quiescent plasmas are perturbed by an impulsive excitation applied to the external electrodes. The result of the perturbation is quasi-linear propagation of a moving pulse within the plasma of the positive column. These results provide the motivation for the consideration in Section IV of a macroscopic theory of the plasma which is developed from the standpoint of transport theory. A linear treatment of the resulting equations leads to some basic conclusions concerning the instability that is shown to exist in the experiments.

Section V discusses the relationships found between the experiments and the theory, while Section VI summarizes the work and makes recommendations for further study.

II. EXPERIMENTS AND OBSERVATIONS

2.1 GENERAL DESCRIPTION OF MOVING STRIATIONS

Moving striations are generally observed in cylindrical discharge tubes containing inert gases. Cylindrical tubes are used because they are simple to construct from glass and are easy to mount and handle. Inert gases are used because they are monatomic and therefore yield more easily to dynamic analysis on the molecular scale.

By far the simplest method of observing moving striations is with a photomultiplier tube and an oscilloscope. A trigger signal for the oscilloscope can be obtained from the electrodes of the discharge tube, and the phototube can be brought close to the discharge after having been provided with a light collimator to provide resolution. Any periodic variation in the light intensity that is accompanied by a like periodic variation in the potential across the discharge tube will appear on the oscilloscope as a regular, periodic function of time. Motion of this periodic pulsation in the light intensity along the discharge-tube axis is translated into motion along the time axis of the oscilloscope display by spatial translation of the phototube in the axial direction.

In order to demonstrate the simplicity of observation and the universal occurrence of this phenomenon, consider the following simple experiment. An ordinary fluorescent lamp of any length is removed from one of the lighting fixtures in the room. It is placed in series with a 2000-ohm resistor and a laboratory 300-volt regulated DC power supply. The supply voltage is increased, a Tesla sparking coil is brought near, ignition occurs, and the current is adjusted to be ~15 ma. An oscilloscope is synchronized by auxiliary electrical connections to the tube terminals. A phototube is placed before the lamp behind a small opaque screen with a collimating slit. Under these conditions, moving

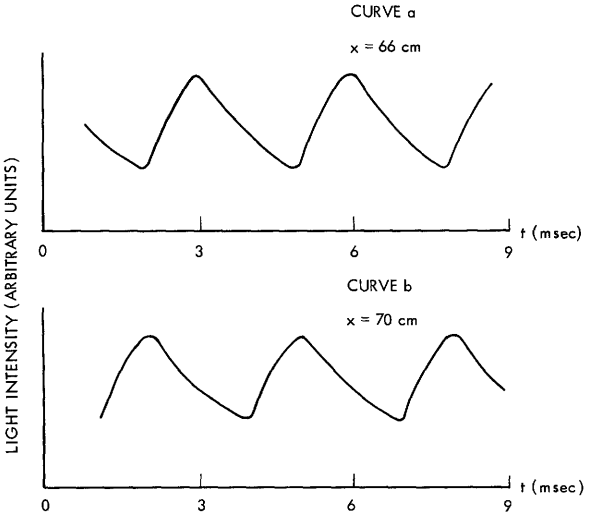

Fig. 1. Variation of light intensity from a fluorescent lamp in DC operation.

striations are invariably present, are observed by the phototube, and are displayed on the oscilloscope.

Figure 1 is a schematic diagram of the approximate wave form actually observed under the conditions outlined above. In curve a, the phototube was 66 cm from the anode. In curve b, it was 70 cm from the anode. As the phototube was moved manually from position (a) to position (b), the peaks were observed on the oscilloscope to move continuously and uniformly from the wave form of curve a to that of curve b, each peak occurring later in time, after the beginning of the sweep, the more closely the phototube approached the cathode.

Since the oscilloscope sweep is initiated independently by the voltage fluctuations at the discharge tube terminals, the movement of the light peaks in time can be interpreted as the movement of a wave of atomic excitation along the tube. In this example, the wave is seen to move 4 cm in 2 msec, which sets the velocity of propagation at 2000 cm/sec. The period of the wave is 3 msec, and accordingly the frequency is 330 cps. Since the velocity is uniform, the wavelength of this traveling wave is 6 cm.

It has been found (see, for example, Stewart[23]) that accompanying these periodic variations in the light emanating from the discharge are also periodic variations in the electron density, electron temperature, longitudinal electric field intensity, terminal voltage, and terminal current of the tube. Excited atoms emit the light observed by the phototube. It is thus quite probable that a wave of ionization also accompanies the light. From the variation in the electric field and the electron density, it is also possible to deduce that there is a variation in the ion density with space and time. Thus it is seen that all of the measurable properties of the plasma are disturbed by the presence of the wave.

To conclude this general description of the observable phenomena, several of the more consistent observations may be summarized here. First, the general appearance of the light intensity is very often that characterized by the schematic trace of Fig. 1. There is a sharp rise in intensity followed by a more gentle decline. The wave form of the light intensity as a function of time is independent of whether the wave is physically traveling toward the anode or toward the cathode. In space it is oriented in its travel, much as a shock wave is oriented, with its sharply rising initial portion facing in the direction of its motion. Hence, that portion of the waveform always presents itself to the phototube first, followed by the more gently sloping trailing edge of the disturbance.

Frequencies at which these oscillations are observed vary according to the conditions of the experiments performed. The range of frequencies is quite restricted, however, extending from several hundred cycles per second to several hundred kilocycles per second. The upper limit of frequencies is still well below the ion plasma frequency at the ion densities normally encountered in glow discharges. For instance, as the current density in a glow discharge in argon is varied from approximately 0.1 ma/cm^2 to 10 ma/cm^2, the plasma frequency varies between approximately 300 kc/sec and 30 mc/sec.

The wavelength of naturally occurring moving striations seems to be associated, either directly or indirectly, with the dimensions of the vessel in which it is enclosed. Wavelengths smaller than the tube diameter are rarely observed and a good average wavelength seems to be several tube diameters. Wavelengths longer than the separation between the electrodes have not been recorded, although, some wavelengths equal to the length of the positive column in argon discharges have been observed during the course of the experiments reported here.

Reported wave velocities range from 10 m/sec to 1000 m/sec. These limits bracket the velocity of sound, which in the gases most used is generally approximately 300 m/sec. An important observation that may be made is that the observed wave velocities have always been bracketed by the drift velocities of the ions and electrons, never being greater than that of the electrons and never being less than that of the ions.

2.2 EXPERIMENTAL APPARATUS

One of the difficulties encountered in the literature concerning the observation of moving striations is the incomplete or vague reporting of the precise conditions under which the experiments were conducted. In this section the measurements required for an adequate description of the operating conditions will be discussed, and the apparatus used in the experimental part of this investigation will be described. The desirability of the detailed measurements will become more apparent from the theoretical discussions in Section IV.

First, it is desirable to use the technique of phototube observation of the discharge to have a fast and reliable method of detection. It has been found by comparison of probe and phototube observations that the electron density wave follows closely the light variations and, therefore, is a good indication of the way in which the electron density is varying.

It is also desirable to be able to measure the electron density, the plasma potential in the radial and longitudinal directions, the wall potential, and the electron temperature. This procedure necessitates the positioning of movable Langmuir probes within the discharge enclosure. Langmuir-probe characteristics may then be taken at several radial and longitudinal positions in the discharge. Reduction of the probe data will then reveal all of these quantities.

The steady-state average values of the terminal voltage and current must be recorded for each observation, as well as the vacuum-system pressure. Also, knowledge of the time variation of the terminal measurements and the leak rate of the vacuum system may be desirable under some experimental conditions.

Finally, details of the external circuit configuration and the nature of the power supply should be carefully noted at each observation.

The design of the first discharge tube used in this investigation incorporated many ideas obtained by evaluating the deficiencies of the apparatus used by others and reported in published works. The main problems have seemed to be complicated geometrical

construction of the tubes and unnecessarily complicated electrode structures. It is clear that any sudden increase in the cross section of the tube anywhere within the discharge space causes an unsteady behavior of any striations generated. Therefore, it is of considerable importance to construct a tube of uniform cross section extending from well behind the cathode to well behind the anode. Any deviation from the uniform cross section, for instance, at exhaust ports or positions where probes enter the main discharge chamber should be carefully constructed to maintain the least disturbance to the continuity of the wall.

In our experimental work, cold-cathode tubes were used exclusively. Hot cathodes, if properly designed, may also be used to observe moving striations. The important principle to be observed, as has been discovered empirically, is to keep the electrode structure of simple geometrical form. In fact, plane electrodes facing one another across an unbroken expanse of tubing of uniform cross section have always yielded the cleanest and most reproducible results. Probably the most unsatisfying part of the classical work done by Donahue and Dieke[15] on moving striations was the unsteady behavior of the striations generated in their tubes. This was probably caused chiefly by the shape of the electrodes that they used. Some of them were cubical in shape, and others were long cylinders.

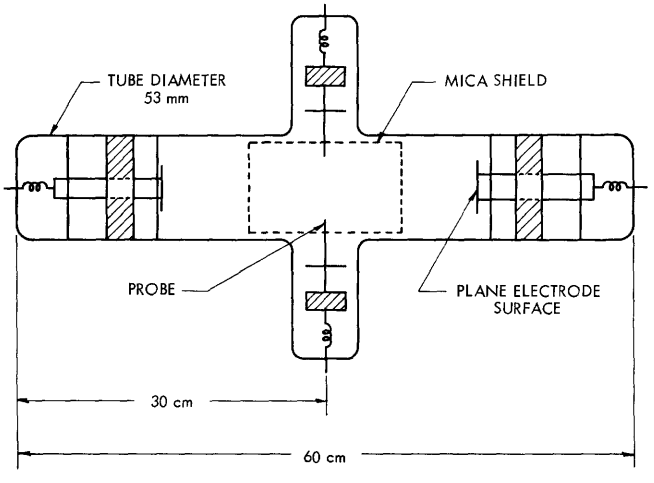

Fig. 2. Discharge tube design.

Figure 2 is a schematic drawing of the initial discharge-tube design used in this research. It proved to be the best of the several that were ultimately used. The tube was 60 cm in over-all length, and it had an inside diameter of 53 mm. Two movable, plane electrodes were situated at either end. Each of these could be moved more than

half of the length of the discharge tube. Located at the midpoint of the cylindrical tube were two movable probes that could be manipulated from the outside with a small magnet. The tubes containing the probes were attached to the main discharge tube at right angles to its long axis; this allowed the probes to be moved radially to a position well beyond the center line of the discharge.

Each of the electrodes was constructed of a flat molybdenum disc, one of them 1 cm and the other 2 cm in diameter, supported by a superstructure of baked-out lava, a thin, soft-iron disc, and a similar stainless-steel disc. The two ferrous metal discs extended to the wall of the tube and supported the electrodes, the iron disc being used to move them with an external magnet. Behind each of the molybdenum discs was placed a mica disc that also extended to the wall of the tube. This was done to delay the onset of arcing of the main discharge behind the face of the electrodes and the supporting structure as the pressure was decreased or the current increased.

The supporting structure for the probes was similar to that of the electrodes except for the mica disc. In order to cover the entrance ports where the probes enter the main discharge space, a large sheet of 2-mil thickness mica was used to form a large cylinder of the same size as the inside diameter of the discharge tube. This was inserted into the main tube. Only small holes large enough to admit the small glass-covered wire probes were then provided in the otherwise smooth mica wall.

Light measurements were made with two Type 931A photomultiplier tubes. One was used as an alternative method of synchronizing the oscilloscope, the other for the actual light measurements. At times, the two were used simultaneously with a dual-trace oscilloscope to obtain rapid measurements of velocity. Each was operated at 850 volts with 100-KΩ resistors between diodes and a 10-KΩ load resistor. Under these conditions, the time constant for the phototube operating into the input capacitance of a Tektronix Type 541 oscilloscope was less than 1 μsec. The amount of light entering the enclosures in which the tubes were contained could be changed by varying the length of the portion of the slit presented to the discharge.

One of the Langmuir probes was a cylindrical piece of wire, 3 mm long and 2 mils in diameter. It was supported by a 10-mil wire that was covered by a thin layer of glass. The other probe, which was positioned opposite the first, was a flat disc of molybdenum approximately 0.1 inch in diameter. It was supported by a structure similar to that of the cylindrical probe and was aligned so that the plane of the disc was parallel to the longitudinal axis of the tube. The side of the disc facing the near wall of the tube was coated with nonconductive aluminum oxide. Only the side facing the center of the discharge actually collected charges from the discharge plasma.

Figure 3 is a schematic diagram of the vacuum system used in the experimental work. The Pirani pressure-measuring gauge was calibrated against a McLeod mercury manometer for each of the gases tested. It was used as the principle pressure-measuring instrument. A manometer was used at the higher pressures, which were beyond the range of the Pirani gauge. The ultimate pressure of the forepump was approximately 1 μ Hg.

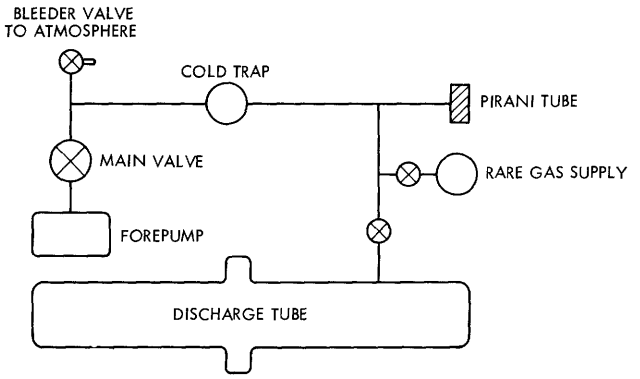

Fig. 3. Vacuum system.

Power was supplied to the bench supporting the discharge tube by two separate sources. One was an unregulated but well-filtered 3000-volt, 300-ma, full-wave rectified power supply driven by a Sola constant-voltage transformer. The other was a series combination of several regulated power supplies capable of supplying 100 ma at 1200 volts with a full-load ripple of 50 mv at 1200 volts.

2.3 PRELIMINARY OBSERVATIONS

Before the first observations made with the system described in the preceding section, the discharge tube was baked out at 500°C. A small electric oven was constructed around the tube on the table supporting the vacuum system. The temperature was increased slowly with the pressure being held below 20 microns to minimize oxidation of the metallic parts. The final temperature was set at 500°C and held there for three days. At the end of that period, the cold trap was filled with liquid nitrogen, and the system was slowly brought to room temperature. The final pressure achieved was 1 micron with the tube at room temperature. Most of the water vapor was considered to have been removed from the tube by this procedure. The electrode parts had been bombed on a separate vacuum system at high vacuum and should accordingly have only had surface contamination at the time of the final bakeout.

After some calibration of the measuring equipment and some trial measurements with the probes, which will be discussed in more detail later, a period of extensive observation of naturally occurring moving striations with the phototube followed. In these measurements, which were carried out in several different kinds of gas under widely varying static conditions within the tube, only the frequency was recorded along with the type of gas and the conditions of static operation. The objective of these tests was to define the regions in which the effects could be most easily observed in the various gases and to pinpoint the gross aspects of the phenomenon.

The chief result of these observations was a distribution of striation frequencies observed for each gas. This distribution has been plotted in Fig. 4 by positioning a small horizontal line at the average observed frequency and a vertical line extending

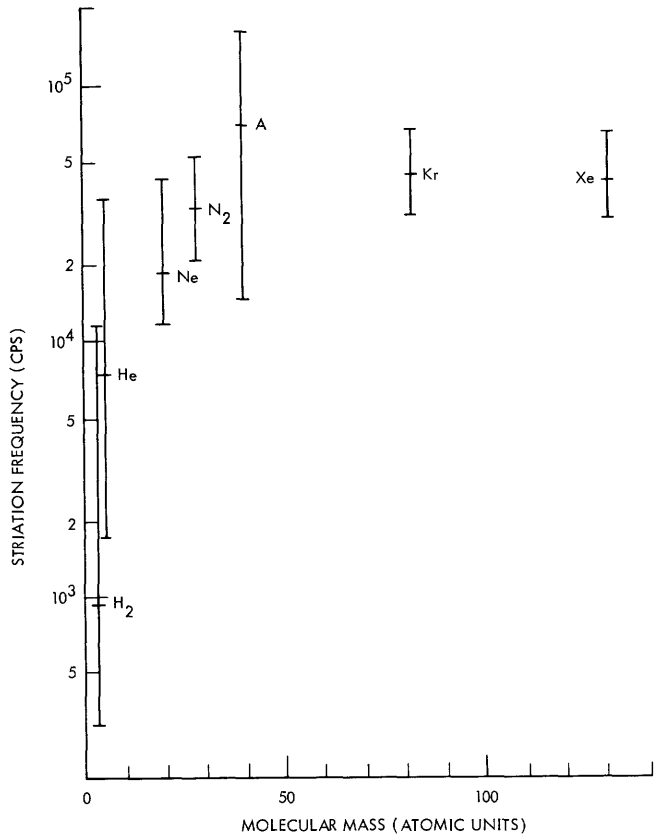

Fig. 4. High, low, and average frequencies of natural striations in various gases.

from the highest observed frequency for that gas to the lowest observed frequency. The various gases are arranged according to their molecular weight. This graph is compiled from a total of 873 separate observations.

One remarkable fact that is immediately apparent from Fig. 4 is that the variation of frequency with molecular weight is opposite to that which would be obtained from an inertial-type, simple, harmonic motion of the ions in the plasma. In this type of motion the particles of the plasma might be visualized as moving under the influence of electrical forces tending to restore the plasma to equilibrium, with inertial reaction forces balancing the restoring force.

In motion of this type, which would be similar to that of a mass attached to a spring or, perhaps more appropriately, a sound wave in a continuous medium, the frequency of oscillation is inversely proportional to the square root of the oscillating mass when the wavelength and/or stiffness of the restoring medium are held constant. As previously stated, the wavelengths of moving striations are fairly constant, and one would expect the electrical restoring force to differ little from one type of gas to the next.

Langmuir and Tonks[10] developed a theory of ion oscillations which has a frequency behavior similar to that of a simple harmonic oscillator. The main features of this theory and its applicability will now be discussed.

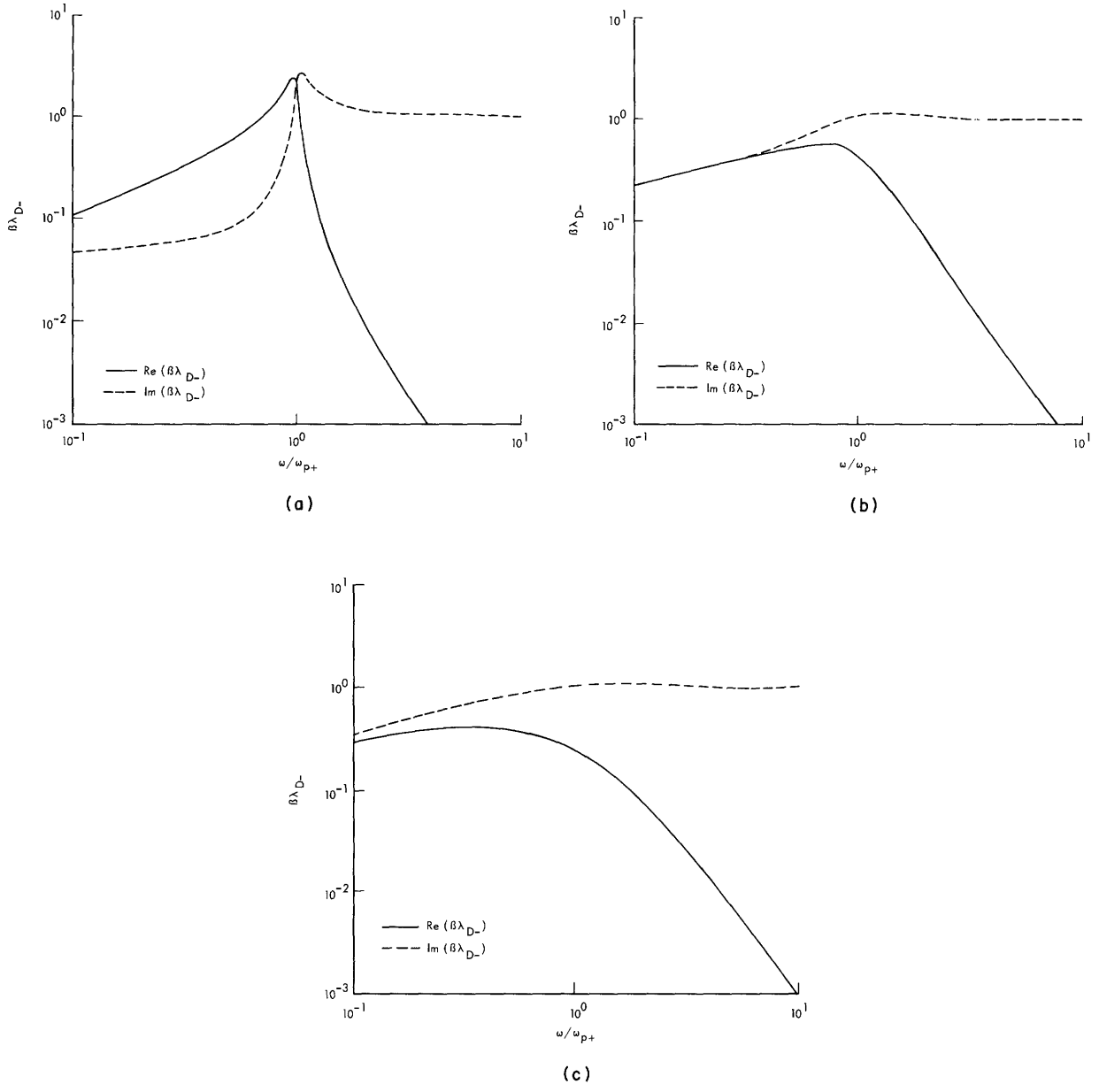

Fig. 5. Solution of Eq. 2: (a) for $\nu_m/\omega_{p+} = 0.1$; (b) for $\nu_m/\omega_{p+} = 1.0$; (c) for $\nu_m/\omega_{p+} = 2.0$.

2.4 ION OSCILLATIONS

Before continuing the discussion of further experiments with naturally occurring moving striations, the present results will be compared with the macroscopic ion oscillations predicted by Langmuir and Tonks.[10] Their results are derived in Appendix A by an alternative method to that used in the original paper. The result obtained when collisions are neglected is the prediction of a soundlike wave propagation that has been called ion sound waves. The characteristic wave speed or ion sound velocity is given by Eq. 1 for the case in which the wavelength is much greater than the electron Debye length.

$$V_{sa} = \left(\frac{\gamma e T_-}{M}\right)^{1/2}, \tag{1}$$

where M is the ion mass, T_- is the electron temperature in volts, and γ is the ratio of specific heats.

At the pressures at which moving striations occur, ion sound waves are damped by collisions with the neutral gas molecules. Langmuir and Tonks did not include collisional damping in their paper; this is done in Appendix B. The result of the analysis is the dispersion (Eq. 2) which predicts attenuation, the amount depending on the ratio of the ion collision frequency to the ion plasma frequency. This relation is

$$\beta^2 \lambda_{D-}^2 = \frac{\left(\frac{\omega}{\omega_{p+}}\right)^2 - j\frac{\omega}{\omega_{p+}}\frac{\nu_m}{\omega_{p+}}}{1 - \left(\frac{\omega}{\omega_{p+}}\right)^2 + j\frac{\omega}{\omega_{p+}}\frac{\nu_m}{\omega_{p+}}}. \tag{2}$$

Figure 5 shows computed solutions to Eq. 2 for values of ν_m/ω_{p+} of 0.1, 1.0, and 2.0, respectively, plotted by Koons[24] and included here for reference. These curves show that when the collision frequency for momentum transfer is equal to or greater than the ion plasma frequency, no propagation of ion sound waves occurs. At low frequencies the propagation is always highly attenuated regardless of the ratio ν_m/ω_{p+}.

For plasmas in a glow discharge, the ion plasma frequency range is approximately 10^6-10^7 sec^{-1}. The collision frequency for positive ions is generally much higher. For example, taking Argon gas at 10 mm Hg pressure, the mobility of the ion in fields likely to be encountered in glow discharges, is 1.37×10^{-2} m^2/volt-sec. If the expression for the collision frequency is

$$\nu_{c+} = \frac{e}{M\mu^+}, \tag{3}$$

then the collision frequency is 1.75×10^8 sec^{-1}. (These data were taken from S. C. Brown.[25]) This calculation is good well within an order of magnitude and clearly precludes ion sound-wave propagation.

The most recent and the most conclusive observations of ion sound waves in plasmas have just been recorded by Alexeff and Neidigh.[26] They used cylindrical and spherical

discharge tubes operating in the range of pressures from 0.01 mm Hg to approximately 5×10^{-4} mm Hg. The plasma densities achieved in their experiments were much higher than those found in the average glow discharge. The factors of low pressure and high plasma frequency placed their experiments in the proper regime for observation of the desired ion waves.

In their discussions, however, they compute the damping effect of neutral gas at higher pressures in terms of an energy-loss argument. They find it to be unlikely that ion sound waves propagate at pressures above 1 mm Hg.

The experimental evidence offered by the increase in striation frequency with molecular mass of the gases used is opposite to that predicted by ion sound-wave theory. The theoretical evidence also shows that ion sound waves are highly damped in ordinary glow discharges. This combined evidence leads to the conclusion that moving striations, observed in glow-discharge plasmas, are not related to ion sound waves.

2.5 DETAILED PROBE MEASUREMENTS

All of the theories previously developed to account for the existence of moving striations in glow discharges have been linearized theories except for that of Stewart.[17] On the other hand, almost all of the experimental evidence points to the conclusion that naturally occurring moving striations are a large-signal phenomenon in the plasma. A basis for this conclusion will be established by an analysis of the results of Langmuir-probe studies of the plasma. In these experiments the time variation of the electron density, the electron temperature, and the longitudinal electric field are inferred from probe characteristics taken when moving density waves were present in an Argon glow discharge.

In the above-mentioned work, Stewart has made similar studies in Argon gas and was drawn to essentially the same conclusions. The results presented here differ from his in two respects that prompt their inclusion at this point. First, the moving density waves that he observed were of low frequency and moved toward the cathode. The ones observed here were of much higher frequency and moved toward the anode. Second, he found that in these slow-moving striations the radial variation of the electron density did not deviate significantly from that predicted by ambipolar diffusion theory. Here the deviation is quite noticeable in the vicinity of the density maximum.

The reason for the widely differing frequencies and velocities observed under similar conditions in these two experiments, as well as the reason for the oppositely directed propagation, is not known. Stewart reports that a disturbance of much higher frequency and very high velocity existed in the tube simultaneously with the low-frequency waves reported. It is quite possible that both positive and negative striations were present in the discharge simultaneously but that the positive striations were of much larger amplitude. One reason for this multiple propagation may have been the unusual electrode shapes that he employed, the anode being a large cylinder and the cathode a right circular cone.

Others[15, 27] have reported simultaneous propagation of waves toward the anode and toward the cathode, and publications abound with observations of either motion observed separately. Motion toward the cathode is invariably at a much lower velocity than that toward the anode with the particle drift velocities being limits between which the velocities range as mentioned above.

The discharge tube and probes described in section 2.2 were used to make the dynamic measurements of the plasma properties. Since the plane probe gave the sharpest break at the electron saturation point, it was used to make the majority of the measurements. Spot checks with the cylindrical probe showed close agreement between the two in absolute values of the quantities measured and very close agreement in the variation of these quantities.

Figure 6 is a schematic diagram of the circuit used to make the measurements. The probe bias was provided by a small, battery driven, potentiometer with capacitive bypass through the capacitor C. Current was measured by recording the voltage developed across a small series resistor R. In addition, the static values of the probe current and voltage were measured.

The original analysis of small d.c. probes made by Langmuir and Mott-Smith[28] is applicable in this situation. In the present experiment the static operating point on the characteristic is fixed by the adjustment of the potentiometer P in Fig. 6. The current-measuring resistor, R, is made small enough to provide negligible change in the probe voltage, V, for rapid changes in the current.

Under certain assumptions, the static theory of the probe predicts that the current to the probe will be given by

$$i = i_{sat} e^{(V-V_p)/T_-}, \tag{4}$$

where V is the voltage of the probe with respect to the anode, V_p is the potential of the plasma next to the probe with respect to the anode, T_- is the electron temperature in volts, and i_{sat} is the saturated electron current. The main restrictions for this formula to hold are that the electron current be much greater than the positive ion current to the probe and that the distribution of electron energies within the plasma be Maxwellian. The first one holds to a good approximation for almost any finite positive probe current because the random ion current to the probe is very small, and the second one is found

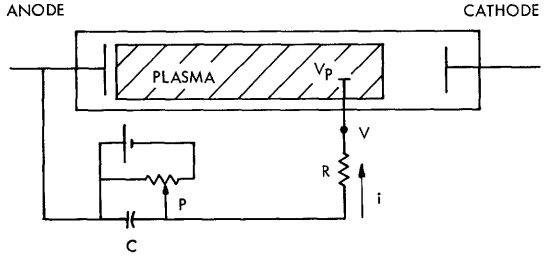

Fig. 6. Schematic diagram of Langmuir-probe circuit.

to be very nearly true by experimental observations.

Equation 4 is valid up to the point where the entire random electron current is drawn by the probe. This occurs at the point where the probe voltage is equal to the plasma potential, at which point under ideal conditions no further current is drawn for further increases in the probe voltage. The ion current may be totally neglected throughout the entire interval of interest because of its exceedingly small value.

When the probe is inserted into the positive column with traveling density variations present, (4) may still be expected to be true under the same restrictions for which it was true in the case of the stationary plasma. The plasma potential and the electron temperature may now be expected to be functions of time. These time variations may be detected by measuring the time-variant deflection of the probe current as the disturbance in the plasma passes into the vicinity of the probe. The plasma potential and the electron temperature may not, however, be directly determined from the deflection but must be obtained by a laborious, point-by-point plot of the current-voltage curve at each instant of time from the observed data. The process of gathering and evaluating the appropriate data will be described next.

Figure 7 is a schematic diagram of a typical current-voltage curve for a Langmuir probe. The region of exponential dependence of current on voltage lies between the voltage limits marked off by the vertical dashed lines. These correspond to the ion saturation current at point A and the electron saturation current at point B. The latter point also defines the plasma potential. The voltage is the probe voltage measured with respect to the anode.

To make a determination of the time variation of the plasma properties, a complete static characteristic is taken all the way from V_A to well into the electron saturation region. At each current an oscilloscope photograph is made of the voltage appearing across the series current-measuring resistor.

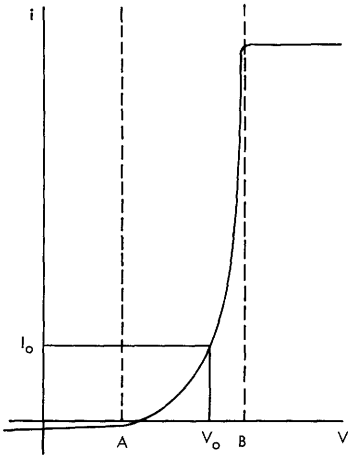

Fig. 7. Probe curve.

Consider what happens to the probe as the plasma potential and the electron temperature vary. When the probe voltage is fixed at the average value V_o, assume that both V_p and T_- change abruptly to new values somewhat removed from the first. If the change from the equilibrium value is rapid and of short duration, only the current to the probe will change. The voltage will be forced to remain constant by the capacitor shunting the probe voltage supply. The current excursion to the new value I_1 will define a single point on a new current-voltage curve which is valid for the new values of V_p and T_-. The development of V_p and T_- in time may be made by varying the probe potential and plotting a complete probe curve for each instant of time during the periodic variation of these quantities. The variation of the electron density may also be determined from the electron saturation-current values at each instant of time, and the variation of the wall potential may also be defined.

An objection that may be raised concerns whether quasi-static equilibrium actually exists so that the static probe theory can be used. In answer to this objection, it may first be pointed out that the time required for the sheath around the probe to be established at the outset is very small. The process, which takes place in the establishment of the sheath, is one of adjustment of the space charge within the sheath to meet the current requirements established by the voltage applied to the probe. The space charge adjusts itself by a withdrawal of electrons by the probe from the sheath if the space charge is inadequate, or by the diffusion of more electrons into the sheath from the plasma if the space charge is too great. In either case, the time required to satisfy the sheath requirement should be of the order of the time taken by an electron to traverse the sheath at thermal speeds.

The space-charge sheath around a probe immersed in a plasma is approximately an electron Debye length in thickness. An equilibrium time may then be established from

$$\tau = \lambda_{D-}/v_{th} = \left(\frac{\epsilon_o T_-}{ne}\right)^{1/2} \left(\frac{m}{eT_-}\right)^{1/2} = \frac{(2)^{1/2}}{2\omega_{p-}} . \tag{5}$$

Since the electron plasma frequency is usually of the order of magnitude 10^{+9} sec^{-1}, any changes in the plasma that occur at frequencies below 1 mc/sec can be treated on a quasi-static basis.

Another argument in support of the use of this technique is that the results are internally consistent. If carefully done, the probe curves plotted in this manner have straight-line regions, when plotted on semi-log graph paper, and the temperatures obtained from the slopes of these curves vary in a regular manner as the wave front sweeps past the probe. The electron densities and plasma potentials plotted from the curves also show similar consistency.

Some practical matters are worthy of mention. In the measurements made here, we found that if the probe were set to draw saturated positive ion current at a relatively high negative probe bias for a short while before each measurement, then the results were more uniform and repeatable. Drawing saturated electron current was also

effective, but not as good as ion current. In the pressure range beyond about 12 mm Hg the plasma potential and electron saturation current were difficult to determine with precision because of significant rounding of the probe characteristic above saturation. Finally, at very low currents the curves deviated somewhat from linearity. This could have been due to changes in the work function of the probe material, or to some geometrical or surface effect. But more likely it was due to positive ion current that was not corrected for in any of the curves. The effect was small and did not invalidate the temperature measurement.

2.6 EXPERIMENT

The experiment outlined here provided the clearest results of any of several others done under similar conditions. The experimental conditions were as follows:

Tube inside diameter, 53 mm
Electrode separation, 22 cm
Gas, Argon
Pressure, 8 mm Hg
Terminal voltage, 580 volts
Terminal current, 8.8 ma
Striation frequency, 52 kcps
Striation wavelength, 10 cm
Striation velocity, 5.2×10^5 cm/sec toward the anode
E/p, 2.5 volts/cm-mm Hg average (longitudinal)
Electron temperature, 1.64 volts average
Electron density, 1.5×10^9 cm^{-3} average.

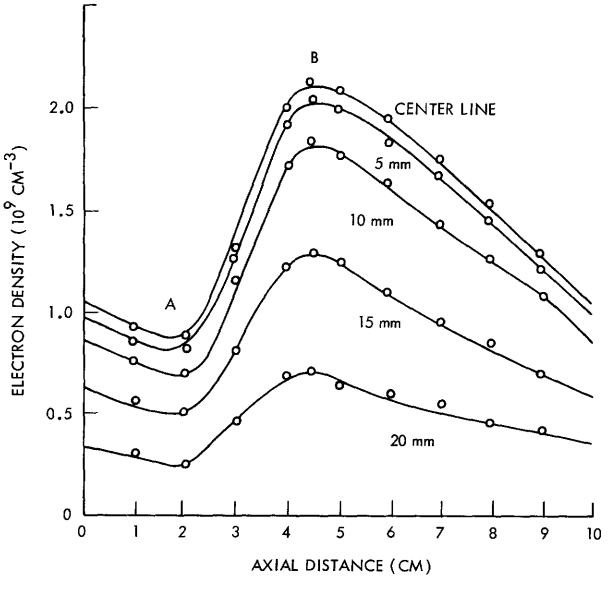

Fig. 8. Electron density vs axial distance for five different radii.

This basic information about the conditions of operation is the minimum amount of useful information that can provide some basis for understanding the problem.

A broad survey of the positive column was made first under the operating conditions listed above. Then the time resolution of the moving striations with the Langmuir probes was made at a specific cross section at various radii. In the survey, which involved taking probe characteristics every centimeter of the length of the tube, the average characteristics were ascertained. The column was found to be free from standing striations, and the plasma potential was a linear function of longitudinal position within the precision of the graphical method (~ ±0.5 volt). The discharge operated continuously in this very stable mode of operation for more than 10 hours with only minor drift in the measured quantities. The drift was probably due to the phenomenon of cataphoresis or "cleanup" in which impurities and gas atoms are removed from the discharge by the current flow and thereby decrease the pressure and increase the cleanliness of the gas.

The time resolution was performed at intervals of 5 mm along a radius located at a point 7 cm from the anode. Figures 8-10 summarize the results of these measurements. The method of presentation is to spread the time variation out in space by multiplying

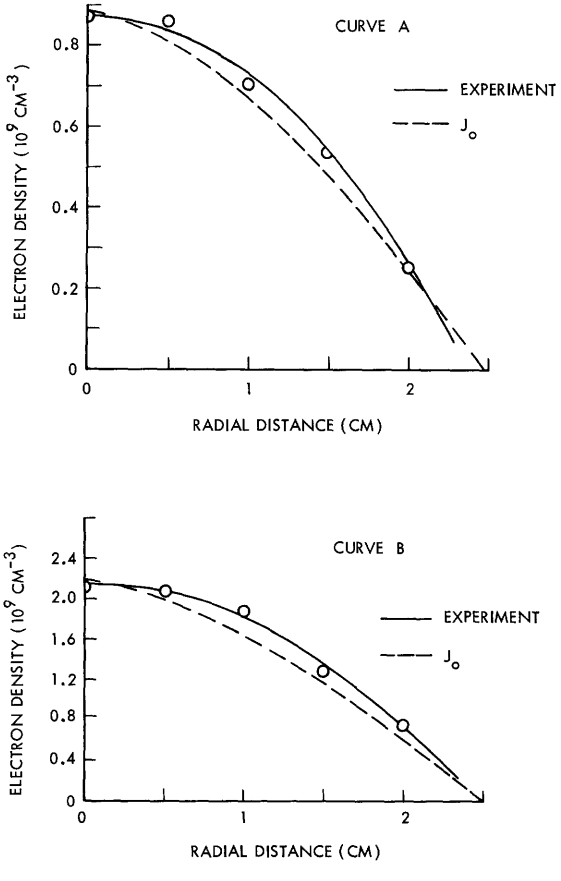

Fig. 9. Radial electron density distribution at wave minimum A and maximum B.

the times of occurrence recorded on the oscilloscope by the wave velocity, which had been found during the longitudinal probe survey and had also been observed separately with phototubes. The wave is oriented as it would be in the tube with the anode on the left, the cathode on the right.

2.7 ANALYSIS OF STRIATION STRUCTURE

Figure 8 is a plot of the electron density as a function of position along the tube for five different radii. The variation of the electron density compared with the average value for radii near the tube axis is sufficient to label the phenomenon as a large-signal one. The radial variation near the peak, which is indicated by curve B of Fig. 9, does not follow closely the zero-order Bessel function, as one might expect. A cut through the minimum at A shows a rather close fit, however. This seems to indicate that, instead of diffusing radially in a zero-order mode near the peak, electrons tend either to move axially as they travel toward the tube walls or to diffuse radially in higher order modes.

The electron temperature shown in Fig. 10 varies only 7.5 per cent from its average value at the tube center line. Other results at the other radii are not shown because they vary little from the value at the center. Aside from the small temperature variation from average, the temperature wave has two other notable characteristics. One is that its peak leads the density peak by approximately 1 cm in the tube. The point of maximum ionization rate can be expected to lie near the peak in the electron temperature curve. Hence the density peak might reasonably be expected to move toward it, that is, toward the anode. The other characteristic is the small value of the temperature gradient in the longitudinal direction. This small gradient indicates that the energy flux that is due to temperature will be small and may be neglected in formulating a theory.

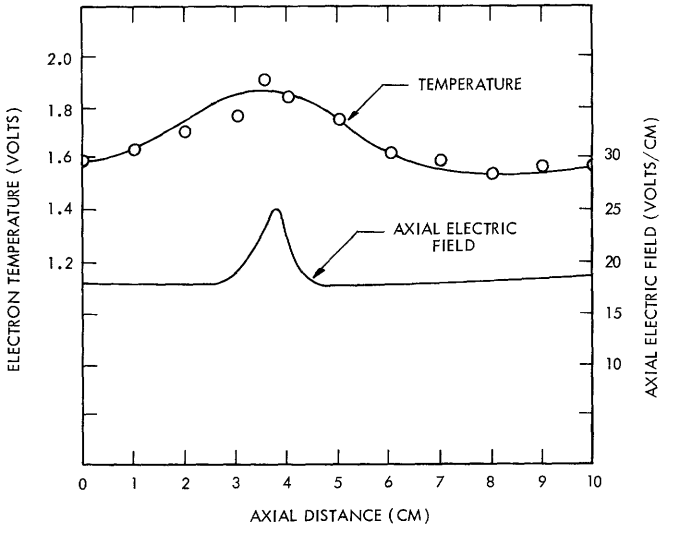

Fig. 10. Axial electric field and electron temperature.

As might be expected, the electric field, shown in Fig. 10 reaches a peak at about the same position as the electron temperature. Because the electric field is derived from the gradient of the plasma potential, its shape is not accurately known. The exact position of the peak and the strength of the field at maximum should have error flags of approximately 0.25 cm and 1.5 volts/cm, respectively, and, therefore, the bump in the field is drawn schematically. The remarkable characteristic of the electric field, aside from its displacement from the peak of the electron curves, is its localized nature. This indicates that there is only significant charge separation near the steeply inclined wave front.

2.8 CONCLUSIONS FROM EXPERIMENTS

We have described some equipment used to measure the gross properties of moving density disturbances in plasmas, and some of the experiments performed with this equipment have been discussed. From this discussion, two major conclusions may be drawn. First, the ion sound-wave theory cannot account for the existence and propagation of naturally occurring moving striations. Second, the characteristics of naturally occurring moving striations cannot be predicted solely from a linearized analysis of the nonlinear governing equations because they are a large-signal phenomenon.

III. LINEAR EXPERIMENTS

3.1 QUASI-STABLE OPERATION

We have shown that naturally occurring moving striations are not a small-signal phenomenon. Instead, they are probably a growing disturbance that becomes limited in its growth and reaches an equilibrium with the walls of the containing vessel. The rate of growth of the instability is rapid because saturation is experimentally observed to occur in the first centimeter of travel for waves traveling toward the anode. For cathode-directed waves, saturation is complete by the time the wave has traversed the anode sheath.[29]

On the other hand, stable regions of operation exist for which moving striations are absent and for which the static theory of the positive column is appropriate. At fixed pressures, these regions consist of ranges of current for which striations are absent. When the geometry of the tube is set and the type of gas to fill the tube selected, the regions of stable operation are fixed. They are subsequently a function only of the pressure and current at which the tube is operated. The positions of the regions of instability and stability are themselves quite stable, but they are subject to some drift, apparently because of ageing of the tube and sputtering of the cathode.

When tubes are used which have a plane-parallel electrode structure that has been well shielded to prevent arcing, the unstable region usually consists of a single continuous range of currents at each pressure. When the electrode structure is irregular, however, the regions in the pressure-current plane where moving striations are observed may be more complex.[15]

The boundary between stable and unstable regions in the pressure-current plane is subject to some hysteresis as the operation is shifted from a stable region to an unstable one and returned by variation of either current or pressure. The onset of the instability, as measured by the spontaneous presence of moving striations, when the operating point is moved <u>from</u> a stable <u>to</u> an unstable region, is usually remarkably reproducible.

At values of current and pressure which place the operation of a glow-discharge tube in a stable region but near the boundary of an unstable region, the plasma of the positive column is in a quasi-stable state. Minute noise fluctuations, which are always present in the plasma, become larger in amplitude, and small, but measurable, random fluctuations appear in the terminal voltage and current. Quite often a periodic flicker appears in the anode glow.[27]

It has been found that a pulsed increase or decrease in the tube current, when the tube is operating in the quasi-stable region, will cause a disturbance to propagate in the plasma. This propagation bears some striking resemblances to natural moving striations, but the nonlinear characteristics of the large-signal phenomenon are absent from the induced disturbance. It is in this quasi-stable region that the experiments to

be discussed now were performed.

The motivation for attempting to excite moving density waves with impulsive excitation came from an experiment reported by Van Gorcum.[30] With rotating mirrors, he observed discharges that were being rapidly switched on and off. During the first instants after ignition, he found that there was a short period of time when no striations existed in the homogeneous positive column. After that, a disturbance propagated away from the cathode, and initiated the continuous propagation of moving striations from the anode toward the cathode during the rest of the cycle. In terms of the two regions of operation, he was transiently initiating the discharge under conditions that placed the operation in an unstable region. During the negative half-cycle of square-wave excitation, the tube was turned off.

We shall give a detailed analysis of some experiments in which short-duration pulses were applied to tubes operating in the quasi-stable regime. The DC operating point was not significantly disturbed by this excitation, because of the extreme brevity of the applied pulse and the low pulse-repetition frequency. The major features of the traveling pulses that were observed will be described in detail, and this will provide the motivation for considering (in Section IV) a linearized theory of the plasma to account for the observed behavior.

Figure 11 shows the typical light pulse observed in the positive column when an impulse current perturbation is applied to the discharge tube in a current region near spontaneous oscillation. The large-amplitude pulse occurs simultaneously throughout the column at the instant when the current impulse is applied. It represents an increase in the light intensity over the average value L_o. The wave packet, which occurs later in time, is found to be a coherent oscillation in the light intensity about the average. The packet itself travels toward the anode with a velocity between 10^4 and 10^5 cm/sec. This velocity will be called the "group velocity" and will be termed negative because its direction of travel is toward the anode, as would be that of a negatively charged particle. The structure making up the wave packet travels in a direction opposite to that of the packet itself, toward the cathode. Its velocity, called the "phase velocity," will be termed positive for a reason similar to that given for the sign of the group velocity. This sign convention conforms to that of the literature on natural moving striations.[15]

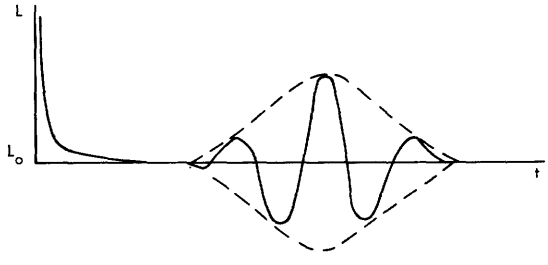

Fig. 11. Light intensity vs time at a fixed position in the positive column.

The assignment of the terms group velocity and phase velocity to the velocity of the packet and the structure of the packet, respectively, is an arbitrary one. The resemblance between the propagation to be described here and linear propagation of

waves in a dispersive medium is so close as to make the designations useful. Also, the theory derived in Section IV will be a linear theory and the terminology will be useful in making comparisons between experiment and this theory.

As well as the unusual property of the group velocity and phase velocity being oppositely directed, this propagation has the characteristic that the group velocity is always greater than the phase velocity by a factor that lies between 2 and 10. Typical wavelengths associated with the structure are of the order of centimeters; this compares closely with that of natural positive striations. It should also be noted that the same relationship between the magnitude of the velocities of natural positive and negative striations also exists.

As the strength of the exciting impulse is decreased either by shortening its duration or decreasing its amplitude, the amplitude of the wave packet changes by a proportional amount. Both the phase velocity and the group velocity are fairly constant throughout their travels and become nonuniform only in the regions adjacent to the electrodes where the plasma density and the electric field are likely to be nonuniform. Both the amplitude variation and the uniform velocities would tend to support the contention that the propagation is linear.

The packet spreads out as it travels axially and its amplitude may decay with distance, remain relatively constant or grow as it makes its way toward the anode. Which one of these gain conditions is encountered is determined by the proximity of the mode of operation to the unstable region. The closer the unstable region of operation, the less attenuation is encountered. When operation is very near the region of instability, operation may occasionally pass over to uncontrolled spontaneous oscillation.

A detailed description of the results of a comprehensive examination of these externally excited density waves will be given here. It will be shown that they are closely related to naturally occurring moving striations and are probably not associated with sound waves in the neutral gas.

3.2 DESCRIPTION OF EXPERIMENTAL APPARATUS

In the series of experiments described here, a cylindrical tube with 3-cm I.D. was used. It was approximately 60 cm long, with a 30-mm ground-glass joint at each end. The main electrodes were attached to wires pressed through glass that was fused to the distal segment of the joints. In this way, the electrodes could be removed, the electrode design revised or the tube cleaned without having to break the tube.

Six small Langmuir probes were placed alternately at 4-cm intervals along the length of the tube, starting 4 cm in front of the anode. Each one could be moved radially to the tube center line. The main electrodes were molybdenum discs, 1 cm and 2 cm in diameter, rounded slightly at the edges to reduce fringing electric fields. Each electrode was supported by wires that were flame-sprayed with aluminum oxide to prevent emission, as was the rear of each electrode.

The tube was attached to the vacuum system shown in Fig. 3 after careful degreasing of all parts. Because of the removable joints, which were sealed with vacuum grease of good quality, the system could not be baked. Tests showed, however, that the behavior of this tube compared well with that of its predecessor which had been carefully baked out. It exhibited moving striations under certain regimes of operation with velocities and frequencies similar to those found in the former tube, and the artificially excited waves observed in the new tube were similar to the ones formerly observed.

Figure 12 shows the circuit used to apply the pulse of current to the tube. The exciter, a Dumont 404 pulse generator, produced a pulse of variable width from 0.1 μsec to 100 μsec with a widely variable prf. The rf choke provided isolation of the DC power supply circuit, and a check of the voltage across R_L resulting from the pulse showed it to be negligible.

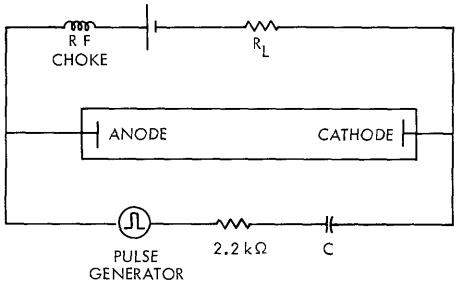

Fig. 12. Schematic diagram of the pulse-excitation circuit.

Observations were made with this apparatus by selecting a current and pressure near an unstable region just outside the range where spontaneous moving striations would appear. Pulses were applied, and the tube current was changed to move the DC operation closer to instability. As instability was approached, the response to the excitation increased in the form of an increase in the light amplitude from the traveling pulse.

Any of the Langmuir probes could also be inserted into the plasma, and the traveling wave could be detected by observation of the current drawn by the probe. If the probe is biased into the electron saturation region of its characteristic and the electron temperature remains constant, changes in the probe current correspond to changes in the electron density in the plasma. Fluctuations in the voltage across the tube could also be monitored during the operation.

3.3 DESCRIPTION OF TYPICAL TRAVELING PULSES IN NEON

Traveling pulses were excited by using this apparatus in hydrogen, helium, neon, argon, krypton, and xenon, but the best observations were made in neon discharges. The following example is typical in gross characteristics of the observations for all gases. The operating conditions were

Gas, Neon
Pressure, 5 mm Hg
Tube current, 1 ma
Tube voltage, 440 volts
E/p, 1.44 volts/cm-mm Hg
Pulsewidth, 30 μsec
Current pulse, 8.6 ma into anode
prf, 120 pps.

Figure 13 is a copy of the oscilloscope traces photographed for this situation. The signal represents light coming from the plasma of the positive column at two different points along the axis of the tube. Trace b was obtained at a position 4 cm closer to the anode than trace a. By moving the photomultiplier tube uniformly from position a to position b, the pulse group is centered uniformly at a later time. This indicates that the pulse group itself is moving toward the anode. On the other hand, as the motion is made from position a to position b, each of the smaller light peaks occurs uniformly at an earlier position in time. This shows that they are moving toward the cathode. The

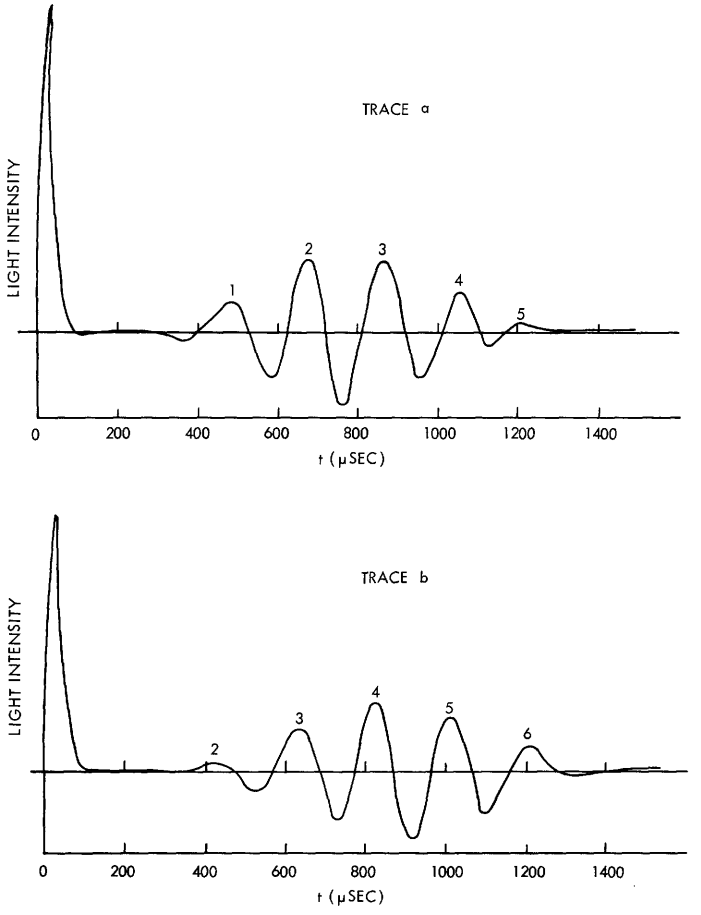

Fig. 13. Oscilloscope traces of traveling pulses in neon.

two velocities may readily be calculated from the diagram:

Group velocity, $V_g = 349$ m/sec

Phase velocity, $V_p = 180$ m/sec.

These two velocities are fairly constant through the travel of the pulse from cathode dark space to anode. Sometimes the velocity changes slightly near these two extremes, usually becoming somewhat slower.

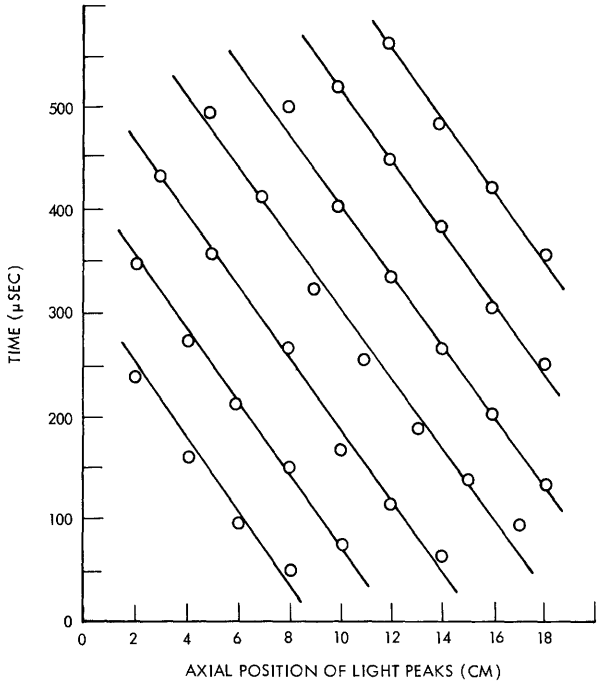

Fig. 14. Positions of light peaks in the traveling-pulse structure as a function of time.

Figure 14 is a plot of the position of the intensity maxima as a function of time for operation in neon at 9 mm Hg and 5 ma. This is a different point of operation from that mentioned above, and yields considerably lower velocities. The average group velocity is $V_g = 256$ m/sec, while the phase velocity, V_p, is 143 m/sec. This diagram shows the traveling-pulse behavior quite graphically. From it a spreading of the wave packet in space and time is seen to exist. One characteristic that it does not show is the decay in the amplitude of the pulse as time increases.

Returning to the time plots of Fig. 13, one finds that the characteristic frequency of the structure of the wave packet is given by the time separation of the amplitude peaks. This frequency is just $f_p = 5.1$ kcps for the former example. The spatial separation between the peaks at any instant of time is defined as

$$\lambda_p = \frac{V_p}{f_p} = 3.5 \text{ cm.} \qquad (6)$$

At any instant of time, the wave packet has a fixed spatial extent that is defined by the distance between the points on the envelope curve where the amplitude is down by a factor of 1/e from its value at the peak.

The total spatial extent of the wave packet cannot be obtained exactly from just two time plots at different positions, as may readily be appreciated from Fig. 14 because it is not exactly symmetrical in both time and spatial directions. A rough estimate can be made merely by counting the number of wavelengths in the group and estimating its length from λ_p. In the above-mentioned case this is just 5 wavelengths or 17.5 cm, which is less than half of the electrode separation of 44 cm.

A striking feature of the time display of the light intensity at a given position is the shape of the envelope containing the structure. It resembles closely a Gaussian pulse. If one were to assume that the traveling pulse is a traveling, diffusing, one-dimensional impulse that was initiated at the instant when the current impulse was applied to the tube, then the diffusion coefficient can be obtained from the oscilloscope plot in the following way. A diffusing pulse has a width at the points where its amplitude is 1/e of the maximum value that is given by

$$2r_o = 4\left(D_M t_o\right)^{1/2} \tag{7}$$

if a one-dimensional diffusion is assumed and if $v_g t_o \gg r_o$. D_M is the desired diffusion coefficient, and t_o is the time between the initiation of the impulse and the arrival of the peak of the wave packet. Solving Eq. 7 for D_M, we obtain

$$D_M = r_o^2 / 4t_o, \tag{8}$$

where r_o is the halfwidth. Substitution of the correct values from Fig. 13 yields $D_M = 0.225\ m^2/sec$.

The important diffusion coefficients are listed below for the discharge that is considered here. The electron temperature was not measured, therefore, it is retained explicitly.

$$D^+ = 7.6 \times 10^{-3}\ m^2/sec$$

$$D_M = 0.225\ m^2/sec$$

$$Da = 0.304\ T_-\ m^2/sec$$

$$D^- = 0.35\ T_-\ m^2/sec.$$

The measured diffusion coefficient would be very close to the ambipolar diffusion coefficient if T_- were approximately 0.75 volt. It would be close to the electron diffusion coefficient if T_- were 0.65 volt. Either of these values is reasonable, but the former seems more likely, because of the relatively large value of E/p.

Comparison of the group and phase velocities of the excited wave in neon at two

different pressures has shown that they differ. Figure 15 is a plot of these two velocities and λ_p as functions of pressure. The average tube current at the points plotted was 4.7 ma; the lowest was 3.5 ma, the highest was 5.0 ma.

At this current, the neon discharge became unstable for pressures much below 4 mm Hg and much above 9 mm Hg. The wavelength remained relatively constant; therefore, the frequency declined with pressure. As the discharge passed over into the unstable regions at the higher and lower pressures, the phase wave tripled in frequency at the transition and became the moving striations of the instability, moving from the anode toward the cathode. The velocity of the moving striations was very nearly that of the phase wave at the transition.

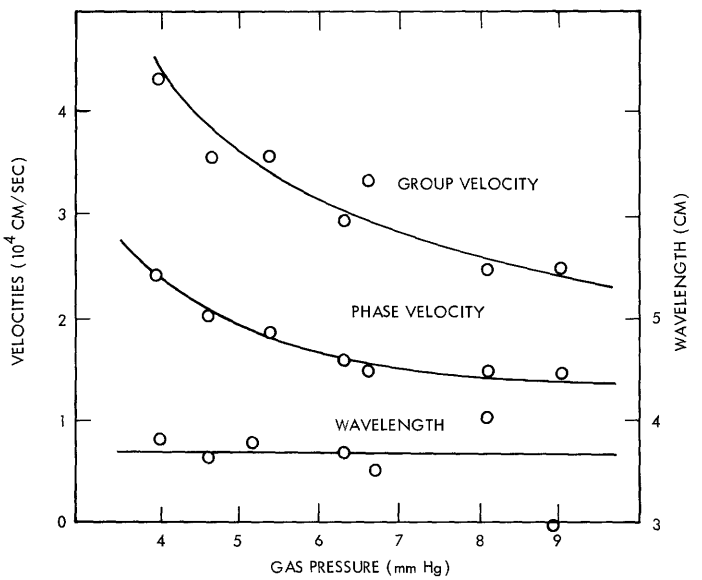

Fig. 15. Velocities and wavelength of externally excited traveling pulses in neon.

Two other characteristics of importance can be seen from Fig. 15. The first is that the onset of the instability at the lower pressure is accompanied by rapid increases in the phase and group velocities, while the wavelength remains relatively stable. At the high-pressure end of the scale, however, where the onset of instability is again imminent, both of the velocities remain relatively constant, while the wavelength varies widely from the average value. The second is that the group velocity increases much more rapidly with decreasing pressure than the phase velocity.

3.4 RESULTS FROM OTHER GASES

Spontaneous moving striations have been found to occur in all of the gases used in the experiments associated with this research. Externally excited waves have also been observed in all of them in some quasi-stable range of tube operation. The results of this extensive study furnish grounds for supposing that the two phenomena are closely

linked and are, in fact, nonlinear and linear manifestations of the same basic mechanism.

The positions of the quasi-stable regions in H_2, He, Ne, A, Kr, and Xe were found to be widely separated in the pressure-current plane. Thus survey measurements in these gases could not all be made at the same pressure, although the results with neon indicated that the traveling-wave velocities depended strongly on pressure. Operation was accordingly set in an arbitrary quasi-stable region where the pulsed behavior was characteristic of that previously described for neon.

In Table I a comparison is made of various velocities of importance in the discharge for each of the gases used under the test conditions.

Table I. Wave, drift, and sound velocities in various gases.

(10^4 cm/sec)	H_2	He	Ne	A	Kr	Xe
V_g	3.78	5.8	2.7	4.5	2.8	2.1
V_p	1.78	0.44	1.4	1.7	0.8	1.2
V_-	200	120	80	75	64	61
V_+	—	1.5	0.38	0.35	0.20	0.18
V_s	14.3	10	4.5	3.2	2.1	1.7
V_{sa}	—	84	38	27	16	9.5
P(mm Hg)	1.5	7.5	6.6	0.85	1.2	1.5
I(ma)	1.2	11.0	1.2	4.8	5.5	7.5

The only close relationship that is evident from Table I is that the group velocities tend to be of the same order of magnitude as the sound velocities, V_s, in the neutral gas. For the heavier gases, agreement within 30 per cent is obtained. Therefore, the role of sound in the neutral gas requires further attention. This is discussed below.

The ambipolar sound velocity, V_{sa}, is calculated on the basis of an electron temperature of 1 volt and γ of 3. These sound velocities were reduced to 27°C, and hence are somewhat below the actual sound velocity at the ambient tube temperature. It is an order of magnitude larger than the characteristic wave velocities.

3.5 SOUND SPEED IN PIPES AT LOW PRESSURES

At low pressures, two viscous effects that are negligible at atmospheric pressure become important in the propagation of sound in small-diameter tubes: an increase of sound speed caused by viscous heating, and a decrease in sound speed caused by viscous friction of the oscillating medium against the walls of the containing vessel. A third effect, arising from the finite heat conductivity of the propagating medium, acts to decrease the sound velocity when the radius of the tube is small compared with the

characteristic length for heat conduction. Accompanying all of these effects is a considerable attenuation, which normally is negligible at atmospheric pressure but becomes important at reduced pressures.

Careful consideration of these effects on the sound speed must be made for the conditions encountered in the small-signal experiments before comparison can be made between the experimentally determined velocities and the speed of sound. It will be found that the increase in sound speed and the attenuation will be negligible for the pressures and frequencies encountered in these experiments. It will be shown, however, that wall friction and heat conductivity may have significant influence on the sound velocity at low frequencies and low pressures. These corrections will be made for the conditions of the experiments in the several gases and will permit a more detailed comparison of the wave and sound speeds.

In Appendix C an approximate expression for the propagation constant associated with a model containing bulk viscous friction is derived after Rayleigh. The result is simply

$$\alpha + j\beta = \frac{2\mu'\omega^2}{3V_s^3} + j\frac{\omega}{V_s}, \tag{9}$$

where μ' is the kinematic viscosity, and V_s is the sound velocity at S.T.P. Figure 16 shows the value of the bulk viscous attenuation constant α for various gases that were used in this investigation. In the plotted expression, the effect of viscous heating on attenuation has also been included. There is no change in the form of the resulting expression; it merely differs from the attenuation of Eq. 9 by a factor of 7/4.[31] This increase in the attenuation can be attributed to the loss of energy by the wave and a resultant heating of the gas through which it is passing. This results in a lossy sound transmission in which the attenuation is increased slightly. It is seen from (9) that by substituting the correct constants for all experimental gases that this increase in sound velocity is negligible to first order in the small expansion parameter $\frac{4\mu'\omega}{3V_s^2}$.

As a basis for the calculation from which Fig. 16 was made, the kinematic viscosity was calculated at 1 mm Hg pressure, and the sound velocity at 0°C. Since the attenuation constant is inversely proportional to the product $V_s p$, the results indicated on the graph can be adjusted for different temperatures and pressures by an appropriate scaling factor.

The dispersion introduced by the viscosity may also be of importance. Greenspan[32] has shown by machine computation of the solution to the complete dispersion equation that when

$$R = \frac{2\beta}{3\alpha} = \frac{V_s^2}{\omega\mu'} < 10, \tag{10}$$

the sound velocity begins to increase monotonically. If one uses the expression for

viscosity derived from kinetic theory,

$$\mu = \frac{5\pi}{32} \rho \bar{v} \lambda_c,$$

and the result from kinetic theory,

$$\bar{v}^2 = \frac{8p}{\pi\rho},$$

then

$$R = \frac{2}{3\pi} \frac{\nu_c}{f}. \tag{11}$$

The significant departure of the sound velocity from its low-frequency, high-pressure value is seen to occur for frequencies greater than about 2 per cent of the collision

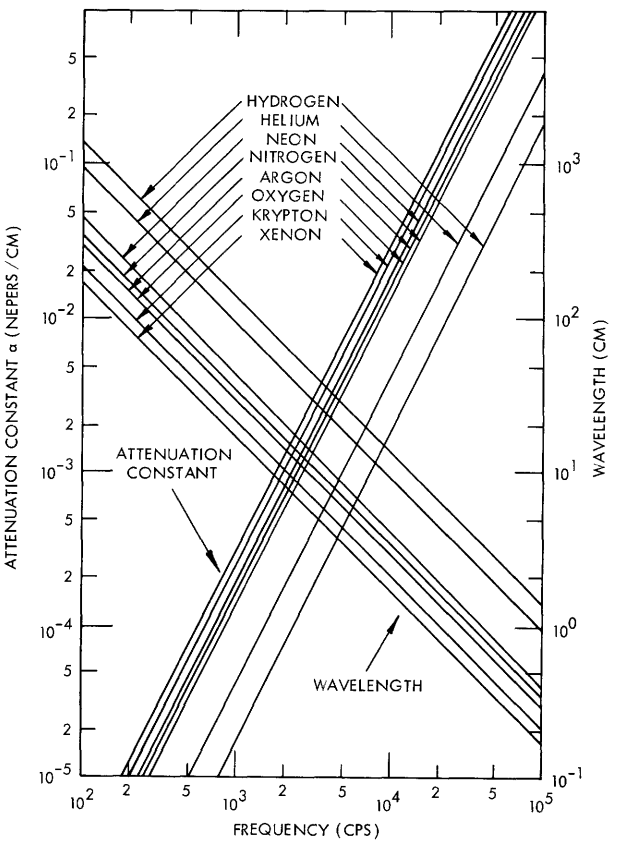

Fig. 16. Attenuation and wavelength of sound in various gases at 1 mm Hg and 0°C.

frequency. In our experiments, the collision frequency was always many orders of magnitude greater than the frequency of any naturally occurring or induced oscillations in the plasma. Changes in the sound velocity because of this particular viscous effect, are thus clearly established as being negligible.

From Fig. 16 it is evident that the attenuation of sound at 1 mm Hg becomes of the order of the length of the discharge tubes used in this investigation in the range of frequencies 10-30 kc for the heavier gases used. Near 100 kc the attenuation length $1/\alpha$ becomes of the order of the diameter of the tubes used. At frequencies below 10 kc sound is transmitted virtually unattenuated by viscous dissipation within the body of the gas.

In Appendix C, the decrease in the velocity of the wave because of viscous wall resistance is discussed. Lord Rayleigh's solution to the problem is presented in Eq. C-5. This is the equation for the approximate value of the sound velocity when viscous wall resistance is included.

Figure 17 shows the velocity decrement that is due to viscous wall resistance. The plotted expression is

$$\frac{\Delta V}{V_s} = -\frac{V_{sV}}{V_s} + 1 = \frac{1}{r}\sqrt{\frac{\mu'}{2\omega}}. \tag{12}$$

Base pressure for the evaluation of μ' was taken as 1 mm Hg, and the tube radius was taken as 1.5 cm.

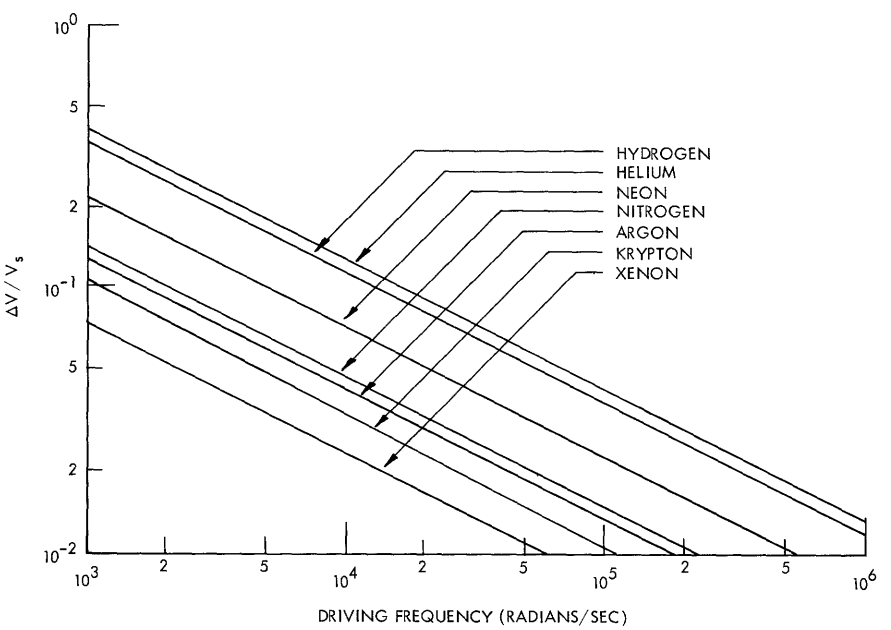

Fig. 17. Velocity decrement resulting from viscous wall friction.

Kirchhoff has shown that the effect of heat conduction to the walls can further decrease the sound velocity below the value at which viscosity alone is considered.[33] The only change in Eq. 12 for the magnitude of the velocity decrement is the replacement of the term $(\mu')^{1/2}$ in the numerator with the term

$$N = \mu' + \frac{V_s}{V_{sN}} - \frac{V_{sN}}{V_s}\nu. \tag{13}$$

The quantity V_{sN} is the Newtonian sound velocity, which is the isothermal value. Stokes has shown that an approximate value for the heat conductivity of a gas is

$$\nu = \frac{5}{2}\mu'. \tag{14}$$

Since the ratio of the adiabatic to the isothermal sound velocity is just $\gamma^{+1/2}$, (13) has the numerical values

$$\begin{aligned} N_m &= 1.82\ \mu' \\ N_d &= 1.55\ \mu' \end{aligned} \tag{15}$$

for gases with monatomic and diatomic molecules, respectively. Therefore, when viscous friction with the walls is important, heat conductivity is also important in modifying the sound velocity. The values of the velocity decrements of Fig. 17 may be corrected for heat conductivity by translating them to higher decrements: 1.82 times higher for monatomic gases, and 1.55 times higher for diatomic gases.

From Fig. 17 it is apparent that at frequencies between 200 cps and 2000 cps the velocity decrement introduced by wall friction in the gases of interest here can be a significant fraction of the total sound velocity at atmospheric pressure. At higher frequencies or at higher gas pressures, the effect tends to become negligible.

Table II shows the decrease in the velocity of sound caused by viscous friction and heat conduction for the conditions of the experiments whose results were summarized in Table I.

Table II. Sound-velocity decrement caused by viscous wall friction.

	H_2	He	Ne	A	Kr	Xe
f (kcps)	11.1	10	4.1	6.7	2.8	3.5
p (mm Hg)	1.5	7.5	6.6	0.85	1.2	1.5
$\frac{\Delta V}{V_s}\left(\frac{Po}{P}\right)^{1/2}$ (%)	6.0	3.5	3.2	4.3	4.1	2.5

Because the frequency content of the pulse is centered at such a high frequency and the pressure is relatively high, it can be seen that the sound velocity decrement is negligible for the experiments that were performed.

3.6 NOTES AND OBSERVATIONS

The examples of externally excited waves given here were drawn principally from experiments performed with neon gas. Examples have been given involving the other

gases at fixed points of operation, but neon was found to be the easiest gas to work with over a wide range of operating points for two reasons. First, the quasi-stable range seems to extend some distance from the boundary of the unstable region in neon; second, the positive column is uniform over a wide range of operation.

In hydrogen and helium generally there are fixed striations extending from the cathode end of the positive column for more than half of the length of the column. The fixed striations have wavelengths almost equal to the wavelengths of the structure within the traveling pulse which may be excited under these conditions. These fixed striations fade out near the anode, and the column becomes fairly uniform there.

When standing striations are present, the propagation of the traveling pulse through them is quite nonuniform, and the pulse shape is wildly distorted, but as the pulse comes into the uniform region of the positive column nearer the anode, it rapidly assumes the general character previously outlined.

In argon, krypton, and xenon, there are usually no standing striations in the discharge tube for operation in quasi-stable regions. The extension of the quasi-stable region in the current-pressure plane is, however, very limited. As operation moves farther into the stable region, the pulse decays very rapidly as it moves toward the anode, the signal fades below the noise level, and the pulse can no longer be detected. Distortion of the traveling pulse also results from overdriving the tube. When the product of the driving-pulse amplitude times its duration exceeds an amount depending on the gas and the operating point, the traveling pulse will be distorted throughout its travel from cathode to anode. The gross characteristics of the pulse are still discernible under these conditions, the pulse group still retains its essential identity, and the structure of the pulse has oppositely directed motion. The velocity of the motion under these circumstances is very unsteady.

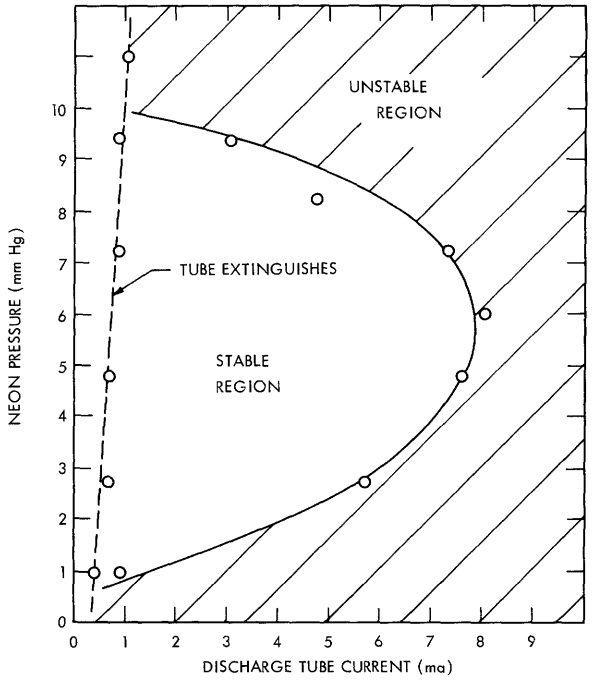

Fig. 18. Lower boundary of unstable region in neon.

In the tube described in section 3.2, when the large electrode was used as the cathode and the small electrode as the anode, the region of stable operation in the current pressure plane was quite simple. It consisted of the clear area to the right of the dashed line which indicates the extinguishing current in Fig. 18. The unstable region extended up to approximately 85 ma at 6 mm Hg where the spontaneous oscillations ceased. The current at which oscillations

ceased at the other pressures tested was more than 100 ma. The upper current boundary was not as reproducible as the lower one shown in Fig. 18, and this may have been due to the evolution of some impurities from the walls of the tube or the electrodes, because of the elevated currents and hence high temperatures.

Argon is the only other gas that had a stable region as simple in shape as that of neon. In argon the region free of spontaneous striations extended to very high currents at some pressures and was also more extensive in the direction of the pressure coordinate. Also, an upper current could not be found which would extinguish the spontaneous oscillations before the designed current limit of the tube was exceeded. This limit could be reached, however, in the larger tube that was described in Section II.

3.7 SUMMARY

The main characteristics of traveling-density waves that have been excited in DC discharges have been outlined. They consist of pulses moving nearly at sound velocity toward the anode, with a substructure moving through the main pulse in the opposite direction. The velocity depends on neutral gas pressure, but has been shown to be fairly uniform as the pulse travels through the tube. Also, the pulse amplitude is directly proportional to the content of the applied impulses.

The uniform velocity, the linear amplitude behavior, and the general shape of the pulse all indicate linear or small-signal behavior of the plasma. As a result of this evidence, a theory of the positive column will be derived in Section IV to describe the operation of the plasma under conditions similar to those outlined here. The relationship between this theory and the present results will be discussed in Section V.

IV. THEORETICAL DEVELOPMENT

A macroscopic theory of the plasma will now be developed in an attempt to clarify the processes at work in a DC discharge plasma. The high collision rate and the steady electric field characteristic of the problem will be taken into account. Ionization will be included in the analysis and will be shown to play a major role in producing an instability in the plasma which can be linked to the spontaneous oscillations that were observed. Some modification of the theory will be shown to be necessary to give adequate qualitative comparison with experiments.

4.1 PREVIOUS THEORIES

Among the linearized theories proposed, the phenomenological approaches of Druyvesteyn[18] and Pekarek[19] are similar. They focus attention on the electron temperature, and the instabilities that they predict are a result of certain arbitrary assumptions about the rate of change of the ionization rate with the electron temperature.

The most complete consideration of the problem has been made by Robertson[20] who uses an intuitive approach. He begins by asserting that the particle motions of all species within the discharge are governed by rate equations of the form

$$\dot{Y} = G - L, \tag{16}$$

where Y denotes the species particle density, G is the production rate for that species, and L is the loss rate. Three equations of this type are written for the ions, the electrons, and the metastable atoms. The neutral atoms are treated as an admixed gas, because of their large number density compared with that of the other species. Diffusion and mobility of the particles are treated as loss mechanisms in the longitudinal direction, and a constant ambipolar diffusion loss term is included for wall losses. Therefore, quasi-static equilibrium is assumed about the known steady-state solution. To eliminate the electric field intensity from the resulting equations, a constant current density is assumed at each cross section of the discharge tube. The current density entered into the equations originally when the approximation was made that the particle current in the longitudinal direction was a result of mobility alone.

Then, Robertson assumes plane-wave solutions to the linearized equations that he derived, and also assumes that the frequency and wave number in the resulting dispersion equation are real. On this basis, two equations are obtained which yield specific numerical values for the wave number and the frequency. These values are assumed to characterize the propagation.

Approximations are necessary to make the analysis of the dispersion equation tractable. In the simplest approximation, the propagation is toward the cathode at the positive ion drift velocity. This is too small to conform to observations by approximately a factor of thirty. The variation of frequency and velocity is found to correspond to the observed variation with E/p; however, the variation of wavelength with

this parameter is reversed. A second limiting approximation, in which diffusion is ignored, is found to be intractable.

The main drawback of this theory is that it is based on unknown functional dependencies of the production and loss rates for each particle species. Also, since the first-order effect of every possible particle interaction within the gas has been included, it is not clear which processes are important and what physical interpretation can be given to the final dispersion equation.

Robertson concludes by listing eight weaknesses in his theory. Any simple consideration of moving striations will undoubtedly have to include a number of restricting assumptions. Yet there is a good deal of motivation to devise such a theory. First, as pointed out in section 1.2, these traveling-density waves are of almost universal occurrence. Their existence must not depend on any specific properties of the gases, but instead must depend on some common properties of all plasmas regardless of the parent gas. For instance, the Ramsauer Effect in argon has often been mentioned as the "cause" of moving striations, but moving striations have been observed in hydrogen, helium, and neon in which the Ramsauer resonance in the electron collision probabilities does not occur. Likewise, non-Maxwellian velocity distributions have also been favored as possible initiators of traveling instabilities. Yet striations occur over such a wide range of operating conditions for the plasma that it seems unlikely that an appeal to a specific velocity distribution for the plasma constituents is the right approach.

The second reason for trying to devise a simplified theory to describe macroscopic traveling-density waves in glow-discharge plasma is that too little work has been done to clarify the processes at work in plasmas at these pressures. High collision frequencies make collisions with neutrals important, but they are difficult to handle. Hence simplified analyses are lacking.

Finally, the discovery that traveling-density variations, which exhibit some linear characteristics, can be artificially excited gives reason for believing that a linearized theory may prove useful.

4.2 DEVELOPMENT OF THE THEORY

The equations of motion of the partially ionized gas of a positive column will be derived from macroscopic first principles. This is done here for two reasons. It will show clearly what approximations are being made, and make clear how the extensions to the theory, which will be proposed later, fit into the development.

As a point of departure, consider the Boltzmann equation[34] which is an expression of particle conservation in six-dimensional phase space.

$$\sum_{i=1}^{3} \frac{\partial}{\partial t} f_j + \frac{\partial}{\partial x_i} v_i f_j + \frac{\partial}{\partial v_i} a_i f_j = \frac{\partial}{\partial t} f_j \Big]_{coll} \qquad j = 1, 2, 3, \ldots \tag{17}$$

where $f_j(\vec{r}, \vec{v}, t)$ is the particle density function in the phase space for the j^{th} species of

particle found in the plasma; a_i is the acceleration in the i-direction experienced by the particles because of external force fields; and $\frac{\partial}{\partial t} f_j \Big]_{coll}$ represents the time change in the density function caused by sudden binary encounters between the particles.

In this development only the three species, electrons, ions, and neutral-gas molecules, will be considered. Other species have been disregarded for various reasons. The negative ions are a minority species with little influence on the motion. The effect of metastable atoms will be assumed to be that of an admixed gas. Other effects on the ionization rate which might be important will be taken care of by approximations concerning the ionization rate.

For the three species of interest, the acceleration vector $\vec{a}$ may be expressed in the following ways:

$$\vec{a}_1 = \frac{-e\vec{E}}{m} - \frac{e}{m}\left(\vec{v}_1 \times \mu_o \vec{H}\right) \qquad \text{for electrons}$$

$$\vec{a}_2 = \frac{e\vec{E}}{M} + \frac{e}{M}\left(\vec{v}_2 \times \mu_o \vec{H}\right) \qquad \text{for ions} \tag{18}$$

$$\vec{a}_3 = 0 \qquad \text{for neutrals}$$

where $\vec{E}$ and $\vec{H}$ are the macroscopic electric and magnetic field intensities. The macroscopic quantities are chosen because the average motion of the particles involved will be all that is finally retained. The magnetic field present will only be that due to the flow of DC and AC currents within the plasma itself. The reaction of these fields on the motion of the particles will be a small effect. Hence the magnetic field may be assumed to be zero in (18).

In many cases the detailed nature of the velocity distribution of the particles as represented by $f_j(\vec{v}, \vec{x}, t)$ is not important in determining the gross behavior of the gas. Indeed, this is the point of view of transport theory, and it has yielded useful results in the study of diffusion, heat flow, and mass transport in neutral gases.

In this development the method of attack will be that of transport theory. At each point in configuration space, the velocity distribution will be assumed to be Maxwellian with a characteristic temperature and a magnitude corresponding to the configuration space density. These densities are defined by

$$n_j(x_i, t) = \int_{-\infty}^{\infty} f_j(x_i, v_i, t)\, d^3v, \tag{19}$$

where $d^3v = dv_1 dv_2 dv_3$.

Under these assumptions, if Eqs. 17 are written in the form

$$B_j = 0,$$

then integrals of the form

$$\int_{-\infty}^{\infty} \vec{v}^k B_j d^3v = 0 \qquad k = 0, 1, 2, 3, \ldots$$

are termed the k^{th} moments of these equations; and the moments have the form of conservation theorems. The notation $\vec{v}^k$ means the k^{th}-order tensor associated with the general tensor product of k velocity vectors.

For instance, if Eqs. 17 are multiplied by $1(=v^o)$ and integrated over all velocities, the $zero^{th}$ moment results. Using vector notation, we have

$$\int \frac{\partial}{\partial t} f_j d^3v + \nabla_{\vec{r}} \cdot \int \vec{v} f_j d^3v + \int \nabla_{\vec{v}} \cdot \vec{a} f_j d^3v = \int \frac{\partial}{\partial t} f_j \Big]_{coll} d^3v, \tag{20}$$

where $\nabla_{\vec{r}}$ is the divergence in configuration alone, and $\nabla_{\vec{v}}$ is the divergence in velocity alone. Through a straightforward application of Gauss' theorem and the fact that $f_j \to 0$ as $v \to \infty$, it can be shown that

$$\int_{-\infty}^{\infty} \nabla_{\vec{v}} \cdot \vec{a} f_j d^3v = \vec{a} \int_{s_\infty} f_j d^2v = 0.$$

Hence (20) becomes

$$\frac{\partial}{\partial t} n_j + \nabla_{\vec{r}} \cdot \left(n_j \cdot \vec{v}_{dj} \right) = \int \frac{\partial}{\partial t} f_j \Big]_{coll} d^3v \tag{21}$$

which is a statement of the conservation of particles per unit volume.

The integrand of the term on the right in (21) is the collision integral. When the collisions are binary and elastic, it can be shown to be identically zero. When collisions are inelastic, ionizations can occur and particles can appear or disappear at any position in space on account of impacts.

In the 3-species gas at moderate E/p, the ionizing collisions are all due to electron-neutral collisions. Also, to a good approximation, electrons have binary collisions only with neutrals. Therefore, it is reasonable to make the approximation

$$\int \frac{\partial}{\partial t} f_j \Big]_{coll} d^3v = \begin{cases} -\nu_i n_1 & j = 3 \text{ (neutrals)} \\ +\nu_i n_1 & j = 1, 2 \text{ (electrons, ions)} \end{cases} \tag{22}$$

where ν_i has the dimensions of ionizations per second per electron. It is related to Townsend's first ionization coefficient by

$$\nu_i = \alpha \left| \vec{v}_d \right|,$$

where $\vec{v}_d$ is the electron drift velocity.

The disappearance of electrons and ions owing to recombination is neglected because of the infrequent close encounters of these two species.[35] The decrease in electron density which is due to attachment is small and merely reduces ν_i. This last process

also creates negative ions that have been neglected because of the improbability of these events.

The statement of the conservation of momentum is the first moment of the Boltzmann equation. The result of taking this moment is

$$\frac{\partial}{\partial t}\left(n_j \vec{v}_{dj}\right) + \nabla_{\vec{r}} \cdot \int \vec{v} \cdot \vec{v} f_j d^3v + \int \vec{v} \nabla_{\vec{v}} \cdot \vec{a} f_j d^3v = \int \vec{v} \frac{\partial}{\partial t} f_j \Big]_{coll} d^3v. \tag{23}$$

It can be shown that

$$\int \vec{v} \nabla_{\vec{v}} \cdot \vec{a} f_j d^3v = -\vec{a} \int f_j d^3v = -\vec{a} n_j$$

by an application of Gauss' theorem.

The collision term multiplied by the mass of one particle may be interpreted as the rate at which momentum is transferred away from a given point in space because of collisions. An example might be an electron colliding with a neutral atom and relinquishing a fraction of its momentum. This momentum disappears from the electron gas at a rate given by the collision frequency for momentum transfer. It is reasonable, therefore, to approximate the collision term for the ions and electrons by

$$\int \vec{v} \frac{\partial}{\partial t} f_j \Big]_{coll} d^3v = \begin{cases} -\nu_{cj} n_j \vec{v}_{dj} & j = 1, 2 \\ +\nu_{c2} n_2 \vec{v}_{d2} & j = 3 \end{cases}$$

For the neutral atoms, the only collisions that transfer any significant momentum to them are with the positive ions. Therefore the collision term for neutrals is very nearly zero. Only a small coupling term to the positive ions exists to a good approximation. For the charged particles the collision term is negative because momentum is lost in each collision with the neutrals, which are nearly at rest relative to the charged particles. Again, collisions between plasma constituents are neglected because of the low-percentage ionization assumed.

The second term in (23) is a vector obtained by the divergence operating on a tensor, the pressure tensor. It is defined by

$$\frac{1}{M_j} \nabla_{\vec{r}} \cdot \int M_j \vec{v} \cdot \vec{v} f_j d^3v = \frac{1}{M_j} \nabla_{\vec{r}} \cdot \overleftrightarrow{P}_j,$$

where M_j is the mass appropriate to the j^{th} species. When the f_j are isotropic and Maxwellian, it can be shown that

$$\nabla_{\vec{r}} \cdot \overleftrightarrow{P}_j = \nabla_{\vec{r}} (n_j e T_j).$$

Applying these simplifications to Eqs. 23, we have

$$\begin{aligned} &\frac{\partial}{\partial t}\left(n_j \vec{v}_{dj}\right) + \frac{e}{M_j} \nabla_{\vec{r}} n_j T_j + \frac{e}{M_j} n_j \vec{E} = -\nu_{cj} n_j \vec{v}_{dj} \qquad (j = 1, 2) \\ &\frac{\partial}{\partial t}\left(n_3 \vec{v}_{d3}\right) + \frac{e}{M_3} \nabla_{\vec{r}} n_3 T_3 = \nu_{c2} n_2 \vec{v}_{d2}. \end{aligned} \tag{24}$$

When the first of Eqs. 24 is divided through by ν_{cj}, we get

$$\frac{1}{\nu_{cj}} \frac{\partial}{\partial t}\left(n_j \vec{v}_{dj}\right) + \mu^j \nabla_{\vec{r}} n_j T_j + n_j \mu^j E = -n_j \vec{v}_{dj} \qquad (j = 1, 2), \tag{25}$$

where

$$\mu^j = \frac{e}{M_j \nu_{cj}} \qquad (j = 1, 2), \tag{26}$$

and $\vec{v}_{dj}$ is the average or drift velocity of the j^{th} species.

In a manner analagous to that used in Eqs. A-7 and A-8, a perfect gas law may be assumed and either adiabatic or isothermal approximations used for the gradient term in (26).

$$\nabla_{\vec{r}} n_j T_j = \begin{cases} T_j \nabla_{\vec{r}} n_j & \text{isothermal} \\ \gamma_j T_j \nabla_{\vec{r}} n_j & \text{adiabatic} \end{cases}$$

The results differ only by

$$\gamma_j = 1 + \frac{2}{\ell_j},$$

where ℓ_j is the number of degrees of freedom of the particles undergoing the motion. Strictly speaking, neither of these approximations is valid for ions or electrons, but only for neutrals. Figure 10 shows, however, that T_- varies little, even in the nonlinear wave motion of natural striations. Hence the isothermal approximation is probably not too bad for this situation.

In any case, the Einstein relation

$$D^j = \mu^j T_j$$

may be used and Eqs. 24 can be written

$$\begin{aligned} &\frac{1}{\nu_{cj}} \frac{\partial}{\partial t}\left(n_j \vec{v}_{dj}\right) + D^j \nabla_{\vec{r}} n_j + n_j \mu^j \vec{E} = -n_j \vec{v}_{dj} \qquad (j = 1, 2) \\ &\frac{\partial}{\partial t}\left(n_3 \vec{v}_{d3}\right) + \frac{\gamma_e e T_3}{M_3} \nabla_{\vec{r}} n_3 = \nu_{c2} n_2 \vec{v}_{d2}. \end{aligned} \tag{27}$$

Note that $\mu^3 = 0$ for neutrals and that $\gamma_3 = 5/3$ is a good approximation for most monatomic gases.

The conservation laws, which have been derived from the most elementary considerations, may now be written as follows.

Conservation of Mass

$$\frac{\partial}{\partial t} n_j + \nabla \cdot \left(n_j \vec{v}_{dj}\right) = \begin{cases} -\nu_i n_1 & j = 3 \\ +\nu_i n_1 & j = 1, 2 \end{cases} \tag{28}$$

Conservation of Momentum

$$\frac{1}{\nu_{cj}}\frac{\partial}{\partial t}\left(n_j\vec{v}_{dj}\right) + D^j\nabla n_j + n_j\mu^j\vec{E} = -n_j\vec{v}_{dj} \qquad (j = 1, 2)$$

$$\frac{\partial}{\partial t}\left(n_3\vec{v}_{d3}\right) + \gamma_3\frac{eT_3}{M_3}\nabla n_3 = +\nu_{c2}n_2\vec{v}_{d2}. \qquad (29)$$

To these may be added Poisson's equation.

$$\sum_{k=1}^{3}\frac{\partial}{\partial x_k}\epsilon_o E_k = \int_{-\infty}^{\infty}(f_2-f_1)\,d^3v = e(n_2-n_1). \qquad (30)$$

These equations represent a simplified picture of the processes that are important in determining particle motions within the plasma. Those processes are drift motions caused by diffusion and mobility, ionization, collision damping, space-charge effects, and inertial reaction.

4.3 COUPLING OF SOUND WAVES

When a gas is weakly ionized, there is weak coupling of the plasma to the neutral gas. This is represented in Eq. 29 by the coupling term on the right of the neutral gas equation. It may be written as

$$\frac{\partial}{\partial t}(n\vec{v}_d) + \frac{\gamma eT}{M}\nabla n = n^+\vec{v}_{d+}\nu_{c+}, \qquad (31)$$

where n^+ is the ion density. One may take the divergence of (31) and substitute (28) to get the wave equation for the transmission of sound in the neutral gas.

$$\frac{-\partial^2 n}{\partial t^2} + \frac{\gamma eT}{M}\nabla^2 n = \frac{\partial n^+}{\partial t}\nu_{c+} \qquad (32)$$

when small signals are assumed for the gas density and temperature. This equation has traveling-wave solutions with the characteristic phase velocity

$$V_s = \left(\frac{\gamma eT}{M}\right)^{1/2} \qquad (33)$$

which is the classical velocity of sound. Note that the excitation of this sound wave is the time rate of the ion density.

Since the percentage of ionization is small, the stimulation of sound waves in the neutral gas by a moving ion density wave can be expected to be small. Coupling in the reverse direction, however, could be considerable. More consideration will be given to the question of sound-plasma interaction in the analysis of the possible role of sound-wave propagation in the linear experiments.

4.4 LINEARIZED ONE-DIMENSIONAL ANALYSIS

When the neutral gas is assumed to be undisturbed, the equations of motion for the plasma may be rewritten from Eqs. 28-30 in the following manner:

$$\frac{\partial n^+}{\partial t} + \nabla \cdot \left(n^+ \vec{v}_{d+}\right) = \nu_i n^- \tag{34}$$

$$\frac{\partial n^-}{\partial t} + \nabla \cdot \left(n^- \vec{v}_{d-}\right) = \nu_i n^- \tag{35}$$

$$\frac{1}{\nu_{c+}} \frac{\partial}{\partial t}\left(n^+ \vec{v}_{d+}\right) + D^+ \nabla n^+ - n^+ \mu^+ \vec{E} = -n^+ \vec{v}_{d+} \tag{36}$$

$$\frac{1}{\nu_{c+}} \frac{\partial}{\partial t}\left(n^- \vec{v}_{d-}\right) + D^- \nabla n^- + n^- \mu^- \vec{E} = -n^- \vec{v}_{d-} \tag{37}$$

$$\nabla \cdot \varepsilon_o \vec{E} = e(n^+ - n^-). \tag{38}$$

Here, a plus sign signifies quantities associated with ions, and a minus sign with electrons. Except for the collision terms, these are identical with the equations of motion set down in Appendix A in dealing with ion oscillations. When the ionization rate is assumed to be a constant, the five equations in five unknowns can be reduced to two equations in two unknowns by the same operations used there. The results are

$$-\frac{1}{\nu_{c+}} \frac{\partial^2 n^+}{\partial t^2} + D^+ \nabla^2 n^+ - \frac{n^+ \mu^+ e}{\varepsilon_o}(n^+ - n^-) - \mu^+ \vec{E} \cdot \nabla n^+ \frac{\nu_i}{\nu_{c+}} \frac{\partial n^-}{\partial t} - \frac{\partial n^+}{\partial t} + \nu_i n^- = 0 \tag{39}$$

$$-\frac{1}{\nu_{c-}}\left(\frac{\partial^2 n^-}{\partial t} - \nu_i \frac{\partial n^-}{\partial t}\right) + D^- \nabla^2 n^- + \frac{n^- \mu^- e}{\varepsilon_o}(n^+ - n^-) + \mu^- \vec{E} \cdot \nabla n^- + \nu_i n^- - \frac{\partial n^-}{\partial t} = 0. \tag{40}$$

Equations 39 and 40 may be linearized by assuming that

$$\begin{aligned} n^- &= n_o + n_1^- \\ n^+ &= n_o + n_1^+ \\ E &= E_o + E_1. \end{aligned} \tag{41}$$

In this notation, the subscripts indicate zero-order quantities which are assumed to be much larger than first-order quantities. Also, plane parallel geometry is assumed, and the equations satisfied by the first-order quantities are

$$\left[-\frac{1}{\nu_{c+}} \frac{\partial^2}{\partial t^2} - \frac{\partial}{\partial t} + D^+ \frac{\partial^2}{\partial x^2} - \mu^+ E_o \frac{\partial}{\partial x} - \frac{n_o \mu^+ e}{\varepsilon_o}\right] n^+ + \left[\frac{\nu_i}{\nu_{c+}} \frac{\partial}{\partial t} + \frac{n_o e \mu^+}{\varepsilon_o} + \nu_i\right] n^- = 0$$

$$\frac{\mu^- e n_o}{\epsilon_o} n^+ + \left[-\frac{1}{\nu_{c-}} \frac{\partial^2}{\partial t^2} + \left(\frac{\nu_i}{\nu_{c-}} - 1 \right) \frac{\partial}{\partial t} + D^- \frac{\partial^2}{\partial x^2} + \mu^- E_o \frac{\partial}{\partial x} + \nu_i - \frac{n_o \mu^- e}{\epsilon_o} \right] n^- = 0. \quad (42)$$

The one-dimensional analysis is carried forward by the assumption of plane parallel wave motion. Under this assumption, solutions of the form

$$n^{\pm}(x, t) = \mathrm{Re}\left[N^{\pm} e^{j(\omega t + kx)} \right] \quad (43)$$

are sought.

The determinantal equation, which is the dispersion polynomial, is quartic in both the frequency and wave number. It is just

$$k^4: 1$$

$$k^3: jE_o \left(\frac{1}{T_+} - \frac{1}{T_-} \right)$$

$$k^2: \left(\frac{1}{\lambda_{D+}^2} + \frac{1}{\lambda_{D-}^2} + \frac{E_o^2}{T^+ T^-} - \frac{\nu_i}{D^-} - \frac{\omega^2}{D^- \nu_c^-} - \frac{\omega^2}{D^+ \nu_c^+} \right) + j\omega \left[\frac{1}{D^+} - \frac{1}{D^-} \left(\frac{\nu_i}{\nu_{c-}} - 1 \right) \right]$$

$$k^1: E_o \left\{ \omega \left[\frac{1}{D^+ T^-} - \frac{1}{D^- T^+} \left(\frac{\nu_i}{\nu_{c-}} - 1 \right) \right] + j \left(\frac{\omega^2}{D^+ \nu_{c+} T} - \frac{\omega^2}{D^- \nu_{c-} T^+} - \frac{\nu_i}{D^- T^+} \right) \right\}$$

$$k^o: \left(-\frac{\omega^2}{D^+ \nu_{c+} \lambda_{D-}^2} - \frac{\omega^2}{D^- \nu_{c-} \lambda_{D+}^2} + \frac{\omega^2 \nu_i}{D^+ D^- \nu_{c-}} + \frac{\omega^2 \nu_i}{D^+ D^- \nu_{c+}} \right.$$
$$\left. - \frac{\omega^2}{D^+ D^-} + \frac{\omega^4}{D^+ D^- \nu_{c+} \nu_{c-}} - \frac{\nu_i}{D^- \lambda_{D+}^2} - \frac{\nu_i}{D^+ \lambda_{D-}^2} \right)$$
$$+ j\omega \left(\frac{1}{D^+ \lambda_{D-}^2} + \frac{1}{D^- \lambda_{D+}^2} - \frac{\nu_i}{D^+ D^-} - \frac{\nu_i}{D^- \nu_{c-} \lambda_{D+}^2} - \frac{\nu_i}{D^+ \nu_{c+} \lambda_{D-}^2} \right.$$
$$\left. + \frac{\omega^2 \nu_i}{D^+ D^- \nu_{c+} \nu_{c-}} - \frac{\omega^2}{D^+ D^- \nu_{c+}} - \frac{\omega^2}{D^+ D^- \nu_{c-}} \right). \quad (44)$$

The form of this polynomial with the dependence of the coefficients on ω and E_o shown explicitly is

$$k^4 + jE_o b_3 k^3 + \left[a_2(\omega^2, E_o^2) + jb_2(\omega) \right] k^2 + E_o \left[a_1(\omega) + jb_1(\omega^2) \right] k^1 + \left[a_o(\omega^2) + jb_o(\omega) \right] k^o = 0. \quad (45)$$

Regarding the form of (45), it is apparent that changing the sign of E_o merely changes the sign of the roots of the wave-number polynomial. Furthermore, changing

the sign of the real frequency ω changes the wave numbers to the negative complex conjugates of the former wave numbers.

These results are in agreement with intuition regarding the wave solutions of the linearized set of equations. The effect of changing the sign of E_o should be the same as that of redefining the direction of the coordinate system. Changing the sign of ω should cause the defined direction of propagation to be changed without changing the form of the solutions.

4.5 ANALYSIS OF SOME SPECIAL CASES

To check the validity of the dispersion polynomial of (44), one may set the steady component of the electric field equal to zero and assume that the ionization rate and the collision frequencies are all zero. Under these assumptions, the collisionless ion sound waves derived in Appendix A should emerge. The assumptions are

$$E_o = 0$$

$$D^+ = D^- = \infty$$

$$\nu_i = \nu_{c-} = \nu_{c+} = 0.$$

Let the following notation be used:

$$\frac{1}{\ell_p^2} = \frac{1}{\lambda_{D-}^2} + \frac{1}{\lambda_{D+}^2}$$

$$\omega_p^2 = \omega_{p+}^2 + \omega_{p-}^2,$$

and note that

$$D^{\pm}\nu_{c\pm} = V_{s\pm}^2 = \frac{eT_{\pm}}{M_{\pm}}.$$

Equation 9 then reduces to

$$k^4 + k^2\left[\frac{1}{\ell_p^2} - \omega^2\left(\frac{1}{V_{s+}^2} + \frac{1}{V_{s-}^2}\right)\right] + \frac{\omega^2}{V_{s+}^2 V_{s-}^2}\left(\omega^2 - \omega_p^2\right) = 0. \tag{46}$$

This is a result obtained previously by Whitehouse,[36] and it describes two modes of propagation which can be assigned to the electrons and to the ions. It does not include the effect of Landau damping and probably is invalid at frequencies comparable to the plasma frequencies.

If we assume that $k\ell_p \ll 1$ and make the approximation

$$\ell_p^2 \cong \lambda_{D+}^2$$

$$\frac{1}{V_{s+}^2} \gg \frac{1}{V_{s-}^2}$$

$$\omega_{p-}^2 \gg \omega_{p+}^2,$$

then (46) reduces to

$$\frac{\omega^2}{\omega_{p+}^2} = \frac{k^2}{k^2 + 1/\lambda_{D-}^2} \quad . \tag{47}$$

This result is identical with the ion sound-wave equation obtained by Langmuir and is identical with Eq. A-15.

Another case of interest is that encountered in glow discharges in which the collision frequencies are very large. In this case, it can be shown by a term-by-term analysis of Eq. 44 that, for frequencies much less than the ion collision frequency, the important terms in the dispersion polynomial are

$$k^4$$

$$+ k^3 j \frac{E_o}{T_+}$$

$$+ k^2 \left\{ \left(\frac{1}{\lambda_{D+}^2} + \frac{E_o^2}{T_+ T_-} \right) + j \frac{\omega}{D^+} \right\}$$

$$+ kE_o \left\{ \frac{\omega}{D^+ T_-} - j \frac{\nu_i}{D^- T_+} \right\}$$

$$+ \left\{ \left(-\frac{\omega^2}{D^+ D^-} - \frac{\nu_i}{D^+ \lambda_{D-}^2} \right) + j \frac{\omega}{D^+ \lambda_{D-}^2} \right\} = 0. \tag{48}$$

The effect of the high collision rate on the original equations is to make the inertial reaction terms in (36) and (37) negligible compared with the terms involving diffusion and mobility. It can be seen that the low-frequency oscillations found in glow discharges must result from particle motion characterized by diffusion, mobility, space-charge coupling, and ionization. It will be shown that ionization can be the primary cause of an instability exhibited by the plasma.

4.6 SOLUTIONS TO THE DISPERSION POLYNOMIAL

Two useful methods were employed in the analysis of the dispersion polynomial for high collision rates shown in (48). In the first of these real values of $\underline{\omega}$ are supplied and the quartic equation in the wave number is solved for $\underline{k}$; in the second method, real

values of $\underline{k}$ are chosen and a quadratic equation for the frequency $\underline{\omega}$ is solved. Physically, the former process corresponds to exciting the plasma sinusoidally at a given position and observing which of the wavelengths is propagated, attenuated, and dispersed, and in the latter, to adjusting a sinusoidal variation of the plasma throughout all space and observing the time envelope of the resulting disturbance at a single point to see how fast the wave attenuates.

When real values of $\underline{\omega}$ are supplied, there are in general four distinct complex values of $\underline{k}$ which satisfy the equation. For realistic values of the various constants associated with the plasma of a positive column, two of the roots represent highly damped modes and may be neglected, while the other two have properties of interest in this investigation.

Figures 19 and 20 show the real and imaginary parts of the wave number $\underline{k}$ for the following assumed constants for argon gas:

$$D^- = 5 \text{ m}^2 \text{ sec}^{-1}$$

$$D^+ = 4.4 \times 10^{-3} \text{ m}^2 \text{ sec}^{-1}$$

$$\mu^- = 8.4 \text{ m}^2 \text{ volt}^{-1} \text{ sec}^{-1}$$

$$\mu^+ = 0.12 \text{ m}^2 \text{ volt}^{-1} \text{ sec}^{-1}$$

$$\nu_i = 10^4 \text{ sec}^{-1}$$

$$n_o = 10^{14} \text{ m}^{-3}$$

$$E_o = -600 \text{ volt m}^{-1}.$$

The plots are made on log-log scales, and the logarithm of the magnitude is the ordinate. The sign in parenthesis shows the sign of the adjacent branch of the curve before the log-magnitude operation was performed. For radian frequencies below $\sim 10^4$ per second, there is propagation for each mode. At frequencies beyond the plasma frequency, the dispersion plots tend toward a diffusion or skin-depth behavior, as would be expected.

The mode represented in Fig. 19 is unstable for frequencies less than approximately 700 radians/sec. This instability is characterized by the fact that the imaginary part of the propagation constant passes through zero and becomes negative at the lower frequencies.

It might be well to comment now that none of the ambiguity found in the dispersion equations of lossless systems is present in the dispersion polynomial under investigation here. The reason is that the solutions to the polynomial are distinct with no complex conjugate pairs. Hence, the question of growing and decaying waves, so carefully considered by Sturrock[37] and others, is not in question. The issue is completely resolved by the functional dependence of the polynomial, as represented by Eq. 45, on $\underline{\omega}$.

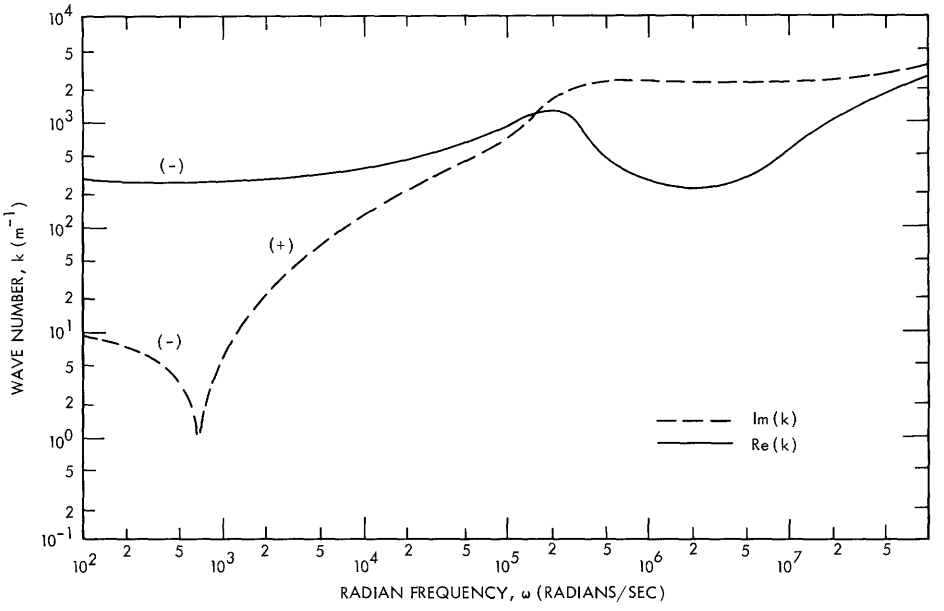

Fig. 19. Unstable solution to the dispersion equation (48).

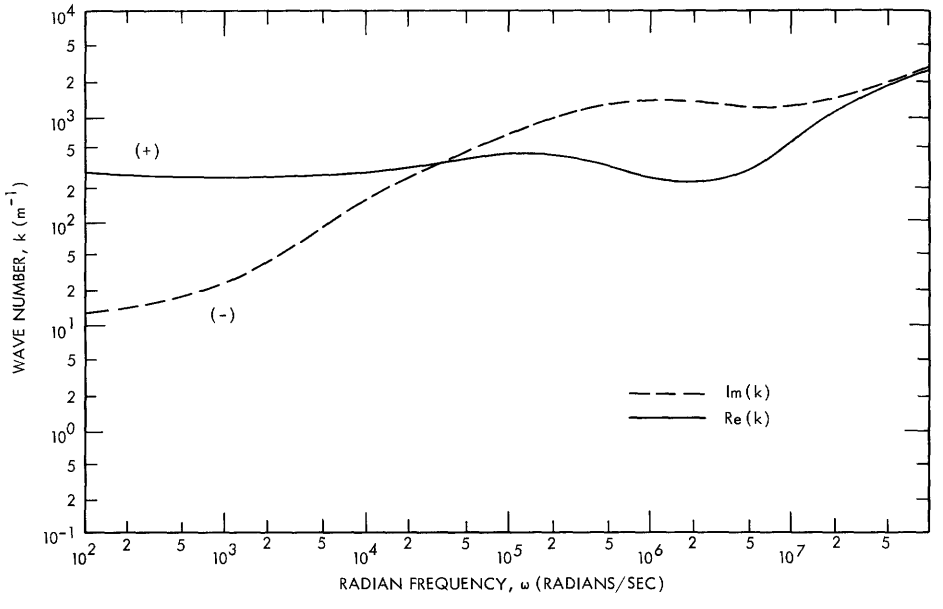

Fig. 20. Stable solution to the dispersion equation (48).

No changes in the algebraic sign of $\underline{\omega}$ or $\underline{k}$ will change the stability of the resulting roots of the polynomial. To ensure stability it is sufficient to establish that the real and imaginary parts of $\underline{k}$ are of opposite algebraic sign. Similarly, in the alternative expression of $\underline{\omega}$ as a function of real values of $\underline{k}$, it is sufficient for the imaginary part of $\underline{\omega}$ to be positive to ensure stability.

Equation 48 may be written in an alternative form:

$$\omega^2 - \left[-\mu^- E_o k + jD^-\left(k^2 - \nu_i / D^- + 1/\lambda_{D-}^2\right)\right]\omega$$

$$- \left[D^+ D^- k^4 + \left(\mu^+\mu^- E_o^2 - \nu_i D^+ + D^- D^+ / \lambda_{D+}^2\right)k^2 - \frac{\nu_i D^-}{\lambda_{D-}^2} - j\mu^+ E_o D^- k\left(k^2 - \nu_i / D^-\right)\right] = 0. \tag{49}$$

Solutions of this equation for real values of $\underline{k}$ should yield values in accord with the interpretation of Figs. 19 and 20. In general, there are two complex-valued solutions for the frequency at each wave number. For practical values of the constants of the plasma, one of the roots is highly damped in the region of wave numbers of interest. The other root shows an instability at low wave numbers.

Figure 21 shows a graph of the solution of Eq. 49 for the same conditions assumed for Figs. 19 and 20. The values of k_o and ω_o correspond to those indicated in Fig. 19, as they should. This shows again that the low frequencies are unstable, the growth rate being given by the negative values of the imaginary part of ω.

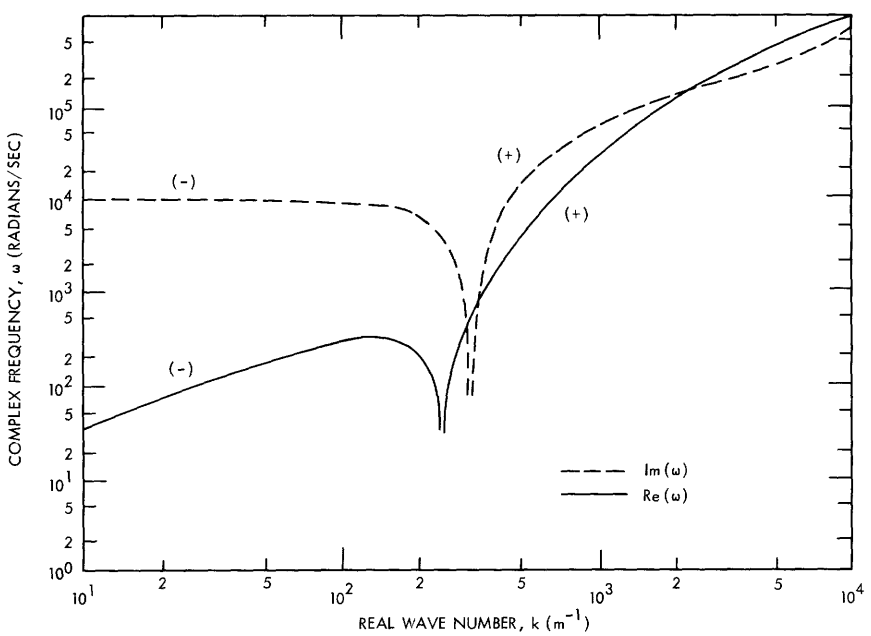

Fig. 21. Solution to Eq. 49 with $\nu_i = 10^4$ sec^{-1}.

For small values of wave number, it can be shown that the following algebraic values for the two roots of (49) are approximately correct:

$$\omega_1 = \frac{-\mu^- E_o D^- / \lambda_{D-}^2}{\nu_i + D^- / \lambda_{D-}^2} k + j \frac{D^-}{\lambda_{D-}^2} \tag{50}$$

$$\omega_2 = \frac{-\mu^- E_o \nu_i k}{\nu_i + D^- / \lambda_{D-}^2} - j\nu_i. \tag{51}$$

Here, ω_1 is highly damped and is associated with the highly damped root mentioned before. The time constant for the damping is just λ_{D-}^2 / D^-; ω_2, on the other hand, has an exponentially growing part with the growth rate ν_i. The implication here is that for very long wavelengths the particle density grows at an exponential rate when a uniform source is distributed throughout all space. This conclusion does not violate physical intuition; in fact, the surprising result is that there is some wave number beyond which diffusion is able to distribute the first-order increase in the number of particles against the first-order losses (again because of the same ionization term) to make the entire system stable.

An algebraic expression for the critical wave number k_o can be derived from Eq. 49 if $\nu_i \ll D^+ / \lambda_{D+}^2$ and if the resulting value of k_o satisfies the relation

$$\sqrt{\frac{\nu_i}{D^-}} \ll k_o \ll \frac{1}{\lambda_{D-}}. \tag{52}$$

In this case,

$$k_o = \left(\frac{\nu_i}{D_a}\right)^{1/2} \times \frac{1}{\left(\frac{\lambda_{D+}^2}{\lambda_E^2} + 1\right)^{1/2}}, \tag{53}$$

where

$$D_a = \mu^+ T_-$$

and

$$\lambda_E^2 = \frac{T_+ T_-}{E_o^2}. \tag{54}$$

Equation 53 implies that if $\nu_i = 0$, the dispersion equation would be stable to infinite wavelength. Figure 22 shows the root corresponding to that of Fig. 21 for identical conditions, except that ν_i has been set equal to zero. In this case, the stability of the system is evident.

Another interesting property of the critical wave number is that it moves to shorter wavelengths and, therefore, to correspondingly higher frequencies as the molecular weight of the positive ion is increased, or as the pressure is increased. This behavior

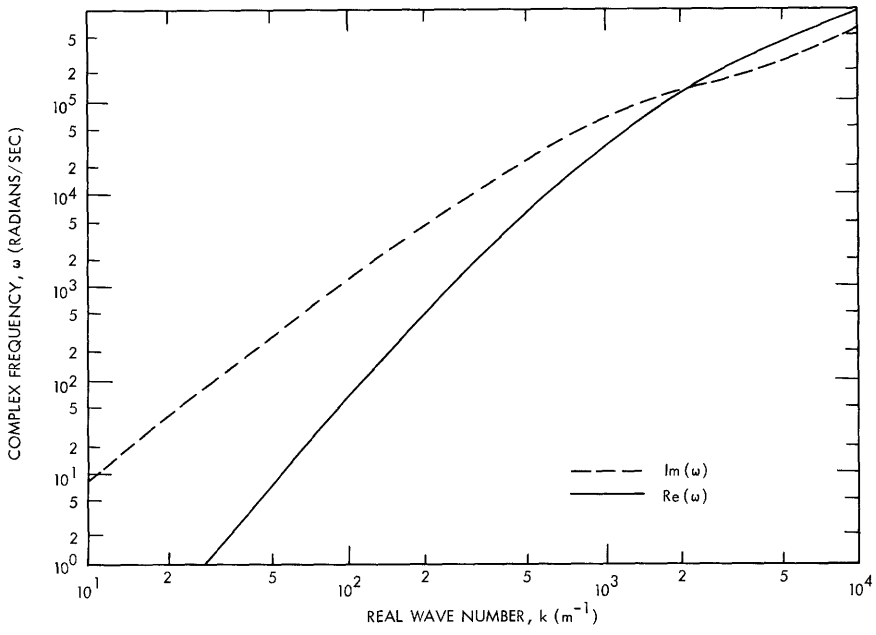

Fig. 22. Solution to Eq. 49 with $\nu_i = 0$.

corresponds to the frequency-mass relations found experimentally and recorded in Fig. 4. The pressure dependence, however, is opposite to that observed. This may be due to the effect of the pressure on the electron temperature, the electric field, and the electron density, all of which play a role in determining k_o.

4.7 AMBIPOLAR DIFFUSION MODE TIME CONSTANTS

Since the ionization rate has been established as the cause of a possible AC instability, it would be proper to inquire whether the ionization should be included in the first-order equations. In an actual cylindrical discharge tube charges are lost to the walls where they combine to form neutral atoms. In the linearized plane-wave solution to the problem thus far considered, this loss has not been considered but may be accounted for in the zero-order solution by assuming that the first-order equations are perturbations about the static ambipolar diffusion solution. But it may be assumed that the first-order solutions also follow the ambipolar law and that the first-order perturbation is in quasi-static equilibrium with the walls. It will be shown that the time constant for the establishment of equilibrium is long compared with typical wave periods and that quasi-static equilibrium in the low-order ambipolar diffusion modes is not possible.

If one assumes a cylindrical geometry with finite, parallel disc ends, the solution of the ambipolar diffusion equation for an arbitrary initial distribution of plasma density is just a linear superposition of solutions of the form

$$n_k = n_{ok} \cos \frac{(2k-1)\pi x}{2L} J_o\left(\frac{z_k}{R} r\right) e^{-t/\tau_k}, \tag{55}$$

where 2L is the length of the cylinder, R is its radius and z_k is the k^{th} zero of the zero-order Bessel function.

The time constant τ_k in (55) is a measure of the time required for the k^{th} mode to decay and is given by

$$\tau_k = \left[D_a \left(\frac{(2k-1)^2 \pi^2}{L^2} + \frac{z_k^2}{R^2} \right) \right] - 1. \tag{56}$$

In general, the time constants get small as the order becomes greater. When $R/L \ll 0.5$ it can be shown that the ratio of successive time constants may be approximated by

$$\tau_k / \tau_{k+1} \doteq z_k^2 / z_{k-1}^2 + \frac{R^2}{L^2} \left[\frac{2k^2}{(2k-1)^2} - \frac{z_k^2}{z_{k-1}^2} \right]. \tag{57}$$

For this expression the following relations are obtained

$$\begin{aligned} \tau_1/\tau_2 &\doteq 5.24 - 3.24(R/L)^2 \\ \tau_1/\tau_3 &\doteq 12.9 \\ \tau_1/\tau_4 &\doteq 24.2 . \end{aligned} \tag{58}$$

The values of τ_1 and the mobilities used in calculating the ambipolar diffusion coefficient for various gases at 1 mm Hg, 30°C, with an assumed electron temperature of 1 volt, are tabulated below.

Gas	Ion Mobility m^2/v-sec	τ msec
Helium	0.726	5.34
Neon	0.298	13.0
Argon	0.116	33.4
Krypton	0.073	53.4
Xenon	0.042	92.3

The velocity of moving striations is usually of the order of hundreds of meters per second. The lengths of the tubes used are generally of the order of tens of centimeters. Therefore, the time required for the disturbance to move the entire length of the discharge tube is approximately 1 msec, or less. In the heavier gases, four or more modes have decay times significantly longer than the period of the wave.

Figure 9 establishes the fact that near the wave front in a natural striation moving at high velocity in argon the particle density is not in quasi-static equilibrium. The

velocities encountered in artificially excited small-signal traveling density waves are of the same order of magnitude, therefore, the same reasoning may also be expected to apply to them.

We conclude that the ionized particle densities generated by the passage of the wave cannot reach equilibrium with the walls in a time that is small compared with the period of the wave, and some mechanism for their accumulation must accordingly be included in the first-order linearized theory. This mechanism is inherent in the inclusion of the ionization term.

4.8 EXTENSIONS TO THE THEORY

The theory of the glow-discharge plasma derived here predicts a long wavelength instability resulting from ionization effects in the first-order perturbation equations. The instability is shown to exist whenever the ionization coefficient is nonzero.

On the other hand, experiments show that the operation of DC discharges is stable under some conditions when the ionization rate is finite. Therefore some modification of the theory is indicated which will provide the damping of long wavelengths indicated by the experiments.

In Section V an evaluation will be made of the correspondence between the results of experiments and the derived theory. One of the main questions that will be explored will be the nature of some possible damping mechanisms and how they might be included in the theory derived here.

V. RELATIONSHIP BETWEEN THEORY AND EXPERIMENT

Several points of similarity exist between the theory that has been derived and the results of the experiments discussed in Sections II and III. These will be discussed here before the principal lack of correspondence between the theory and the experimental observations is dealt with in detail.

The theory predicts a low-frequency and long-wavelength instability in a plasma under conditions similar to those encountered in the positive column of a DC discharge tube. It has been shown that the plasma is unstable for all wavelengths greater than that characterized by the wave number k_o. Equation 53 gives an approximate expression for the critical transition wave number under conditions likely to be found in glow discharges. If

$$\lambda_{D+}^2/\lambda_E^2 \ll 1, \tag{59}$$

then the expression for k_o is approximately

$$k_o \cong (\nu_i/D_a)^{1/2}. \tag{60}$$

If the discharge is assumed to be in static equilibrium in a cylindrical tube, then ambipolar diffusion theory predicts that the equilibrium ionization is given by

$$\nu_i = D_a/L^2, \tag{61}$$

where

$$L = R/2.405 \tag{62}$$

is the diffusion length for the vessel, and R is its radius. The critical wave number is then

$$k_o = 2.405/R, \tag{63}$$

and the associated wavelength is

$$\lambda_o = 2.61\ R. \tag{64}$$

In experiments with nonlinear moving striations, which are occurring spontaneously, the wavelengths encountered in experiments are usually somewhat longer than the critical wavelength λ_o. For example, in the probe experiment in argon outlined in section 2.6, the measured wavelength was 10 cm. The radius of the tube was 2.65 cm which makes the predicted critical wavelength 6.95 cm.

In the linear experiments, the wavelengths associated with the structure of the excited pulse are generally shorter than the critical wavelength. For example, the linear experiments in neon were conducted in a tube of 1.5-cm radius. The graph of Fig. 15 shows that the average wavelength of the pulse structure is 3.6 cm as compared

Table III. Wavelengths of pulse structure.

Gas	Wavelength (cm)
H_2	1.61
He	0.44
Ne	3.41
A	2.54
Kr	2.86
Xe	3.43

with 3.9 cm for the calculated critical wavelength. Table III shows a summary of the measured wavelengths found for the various gases in the 1.5-cm radius tube. These wavelengths correspond to the ratio of the phase velocities found in Table I to the corresponding frequencies found in Table II.

The linear experiments should correspond more closely to equilibrium conditions than the argon experiment, and the agreement between the observed wavelengths and the critical wavelength is correspondingly closer. Another notable feature of Fig. 15 is the relative constancy of the wavelength over a wide range of pressures. Since the critical wavelength is independent of the pressure for the approximation expressed in the inequality (59), this may also be claimed as a similarity between the experimental results and a prediction of the theory.

If the ionization rate is not assumed to be the equilibrium value given by (63) but is assumed to depart from the equilibrium value, by the argument outlined in section 4.8 concerning the time constants for ambipolar diffusion, then k_o becomes a function of E/p. ν_i increases somewhat more rapidly with E/p in the range of E/p of interest than does D_a, hence k_o will be a slowly increasing function of E/p.

Figure 21 shows that the real part of ω increases very rapidly with small increases in the position of k_o. Hence, the group velocity and the phase velocity both increase with increases in E/p. This result corresponds with the results of the linear experiments in neon in which the pressure was varied and both the phase velocity and the group velocity were found to increase as the pressure was decreased. It is well known that natural striations also increase their velocity as E/p increases.

Finally, there are two pieces of evidence from the linear experiments that support the contention expressed in section 4.4 that the coupling of energy from the ion wave to the neutral gas would be insufficient to excite an appreciable sound wave in the neutral gas. First, the pulses excited are shown to have no soundlike character. Their characteristic velocities do not generally correspond to the sound velocity; furthermore, these velocities change with pressure. Second, the pulse excited always travels in the

preferred direction toward the anode. In some of the later experiments, the excitation scheme shown in Fig. 12 was changed so that the excitation was applied between the anode and a probe. Pulses were found to be initiated at the probe and would travel only in the direction toward the anode. When the excitation was applied between the cathode and the probe, the pulse was initiated at the cathode end of the positive column and traveled toward the anode, moving past the probe in the excitation circuit and disappearing into the anode sheath.

Each of the foregoing characteristics describes certain aspects of the theory which have some similarity to achieved experimental results. There is one major departure of the theory from the experiments, and that is persistence of the long-wavelength instability mentioned at the end of Section IV. It is evident that the reason for the instability at long wavelengths is the inclusion of a constant ionization rate in the first-order perturbation equations without provision for some loss mechanism.

There are two possible methods of attack in attempting to modify the defining equations to eliminate this situation. The first is to return to the point in the derivation of the equations at which the constant ionization rate is assumed and attempt to handle the collision integral in a more rigorous way. Then the derived equations would be solved in the coordinate system appropriate to the geometry rather than in a plane geometry. The boundary conditions would automatically include the losses.

A more practical method of dealing with the problem is to include arbitrarily a damping mechanism by hypothesis and to base this inclusion on some plausible, phenomenological reasoning.

5.1 LONG-WAVE DAMPING

Previous discussion of experiments has shown that there are three recognizable domains of operation for glow-discharge tubes. In one region the tube operates in a very stable manner, and the steady-state theory of the positive column accurately describes the operation. In the second region, the positive column is in a quasi-stable state in which small but readily detectable disturbances within the plasma can propagate and even grow in amplitude. In the third region, there is spontaneous oscillation and traveling density waves of large amplitude occur.

The linearized theory considered in Section IV has shown a low-frequency instability that is present whenever the ionization rate is constant and nonzero. It is, therefore, apparent that some damping mechanism must be at work at the lower frequencies. Furthermore, the strength of the damping must depend on the DC operating conditions of the tube in order that the three regions of operation listed above should exist.

Considering the form of the dispersion equation shown in Fig. 21, one might attempt to construct some prototype dispersion relations by modifying those obtained earlier to correspond with observations to obtain the three types of behavior, stable, quasi-stable, and unstable. Figure 23 is an example of how the modified dispersion equation could appear for the three mentioned conditions. Figure 23a represents low current operation

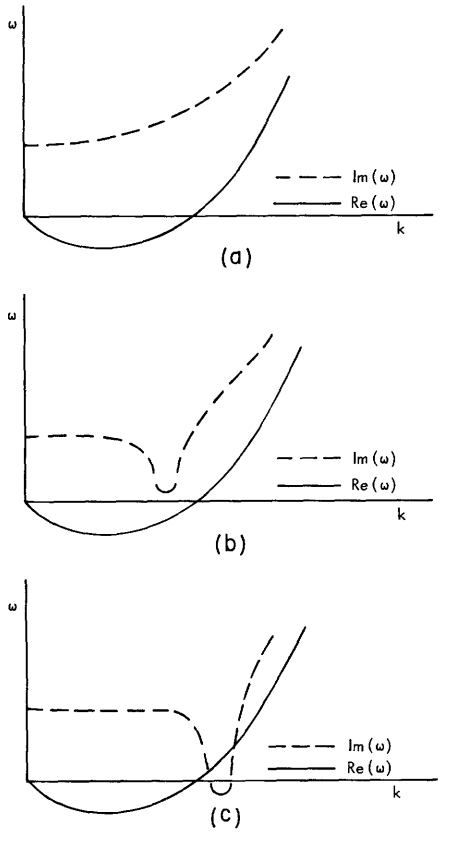

Fig. 23. Prototype dispersion equations for (a) stable, (b) quasi-stable, and (c) unstable conditions.

in argon, for example, with the plasma extremely stable. Figure 23b represents operation near an unstable region where an impulse of current would produce a wave packet with a positive group velocity ($d\omega/dk > 0$) and negative phase velocity. Wave numbers far from the preferred wave number at the minimum in $I_m(\omega)$ would be highly damped. Figure 23c represents a solution to a form of the dispersion polynomial that is applicable to the onset of the instability that would ultimately manifest itself as naturally occurring moving striations. The wave number near the minimum in $I_m(\omega)$ would be most highly unstable and would fix the wave numbers most likely to be encountered in the ensuing traveling waves.

Three phenomenological hypotheses which may be considered to account for the required damping are: (i) increased diffusion losses to the walls at the lower frequencies; (ii) electric field-dependent ionization; and (iii) spatially delayed or nonequilibrium ionization. The last two will be discussed in some detail in the next section. The first is proposed here as an obvious alternative.

5.2 VARIABLE IONIZATION RATE

The rate of ionization in all gases is a function of E/p. In fact, the dependence is exponential in much of the region of operation of most glow discharges (see Brown[38] for argon dependence). This means that the ionization rate is enhanced wherever the E-field is increased and is diminished wherever the field drops below the average value.

If one assumes that the equilibrium ionization rate is a smooth function of electric field and expands it in a Taylor's series about its quiescent value, then it may be approximated to first order by

$$\nu_i = \nu_{io} + \nu_i' E_1, \tag{65}$$

where ν_i' indicates the derivative of the ionization rate with respect to electric field evaluated at the equilibrium field value E_o.

When this value of ionization is substituted in the equations of motion (42), the result is the addition of two constant terms to Eq. 49. The final form of the resulting dispersion

polynomial is just

$$\omega^2 - \left\{\mu^- E_o k + jD^-\left(k^2 + 1/\lambda_{D-}^2 - \nu_{io}/D^-\right)\right\}\omega - \left\{D^+D^-k^4 + \left(\mu^+\mu^- E_o^2 + D^+D^-/\lambda_{D+}^2 - D^+\nu_{io}\right)k^2 - \nu_{io} \times D^-/\lambda_{D-}^2 + \frac{\mu^- E_o \nu_i' T_+}{\lambda_{D+}^2} + jD^-\mu^+ E_o k\left(k^2 - \nu_{io}/D^- + \nu_i' T_+/\mu^+ E_o \lambda_{D+}^2\right)\right\} = 0 \quad (66)$$

Figure 24 is a solution to (66) for exactly the same conditions as were used for Fig. 20 except that the damping of the wave resulting from enhanced ionization is included. It is

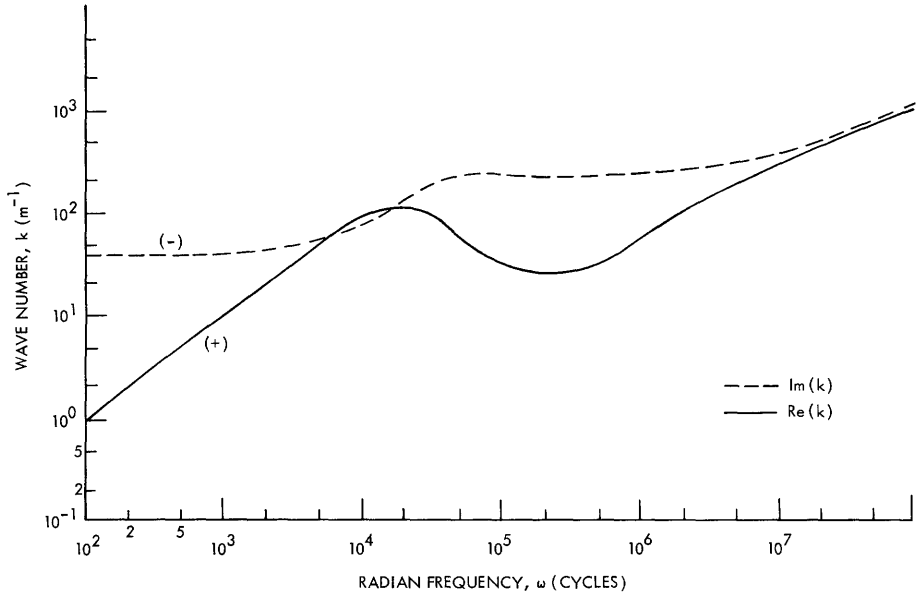

Fig. 24. Solution to Eq. 74 with variable ν_i.

apparent that the damping provided is not of the type sought, but it can cause all propagation at the lower frequencies to cease in the manner of Fig. 23a.

This result has been obtained for conditions of operation which were measured in the laboratory on a tube operating in an unstable region. It would seem that this result would be sufficient reason for abandoning the derived theory at this point and searching elsewhere for the mechanism of moving striations. There are two reasons why this would be premature. First, it may be that the assumption of equilibrium, which is inherent in the use of the curves for Townsend's first ionization coefficient, is not valid. The question of nonequilibrium ionization will be discussed, and its possible role in producing long-wave damping also has a bearing on this discussion.

Second, even if the assumption of equilibrium ionization is valid, minute traces of impurities may have altered the shape of the curve for the particular experiment from

which the data were taken. As a comparison of the effect of traces of impurities on the dependence of ionization rate on E/p, the example of neon-argon mixtures is cited. Traces of argon in neon not only change the slope of the curve drastically, but can change the ionization rate by several orders of magnitude (see Brown[39]).

5.3 NONEQUILIBRIUM IONIZATION

Another possibility for the damping mechanism is to assume that the electrons, which are newly created by ionization, are not in equilibrium with the local electric field but take some time to reach this equilibrium. In this time they will have drifted some distance in the electric field, thereby providing a preferred wavelength for their ionizing effect.

The experimental evidence, on the other hand, is that the electrons are in energy equilibrium with the local electric field. Figure 10 shows that the electron temperature reaches its maximum at the same position as the point where the electric field has its maximum. In order to determine whether this result is reasonable, the instantaneous energy of an electron drifting in a uniform electric field will be derived. It will be shown that under glow-discharge conditions, electrons can drift a considerable distance before coming to equilibrium with the applied electric field at pressures below 1 mm Hg.

Consider the energy du gained and lost by an electron in drifting a distance dx in an electric field E.

$$du = E\,dx - fu\,\frac{\nu_c}{v_d}\,dx, \tag{67}$$

where $\underline{f}$ is the fraction of the energy lost at each collision. If it is assumed that the electron drift is controlled by mobile flow, then

$$v_d = \frac{eE}{m\nu_c} \tag{68}$$

and (67) can be transformed to

$$\frac{du}{dx} = E - \left(\frac{2f}{E\lambda^2}\right) u^2. \tag{69}$$

The equilibrium energy is achieved when the derivative on the left of (69) is zero and is obviously

$$u_f = E\lambda/(2f)^{1/2}. \tag{70}$$

Equation 69 can be normalized by letting $\bar{u} = u/u_f$ and by letting $\bar{x} = 2(2f)^{1/2}\,x/\lambda$. The resulting equation is

$$d\bar{u}/d\bar{x} = \frac{1 - \bar{u}^2}{2} \tag{71}$$

and the solution to this equation is

$$\bar{x} = \ln\left(\frac{1+u}{1-\bar{u}}\right) \tag{72}$$

when the electron is assumed to start from rest.

Figure 25 is a graph of the normalized solution to Eq. 71. It shows that the electron reaches equilibrium for all practical purposes in approximately five of the normalized

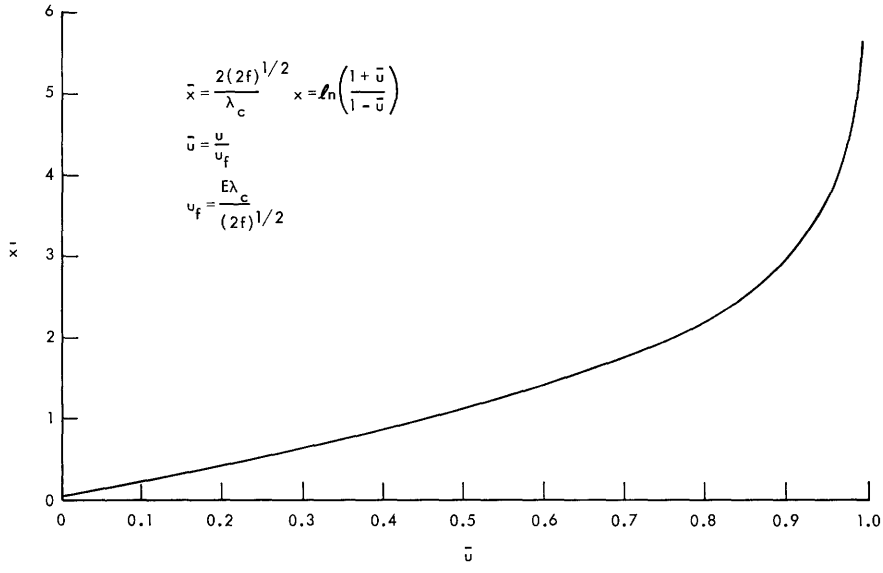

Fig. 25. Normalized distance required for energy $\bar{u}$.

lengths. Table IV shows the expected distance of travel of an electron assumed to lose 2m/M of its energy per collision in a gas at a pressure of 10 mm Hg. Its mean-free path was calculated on the basis of an average temperature of 1 volt. In most gases it is seen by this simple theoretical analysis that the distance traveled by the electron to reach equilibrium is small compared with the wavelengths of interest in all of the gases except argon. The theory does not take into account nonuniform electric fields and the effect of the Ramsauer maximum in the probability of collision.

Table IV. Distance of travel of an electron in a gas.

Gas	Distance to 0.9 u_f (mm)
Hydrogen	0.8
Helium	2.6
Neon	3.3
Nitrogen	6.4
Argon	57.8

5.4 GENERAL ROLE OF IONIZATION

Some insight may be gained into the form the modification to the defining equations must take by considering the following approximate solution of the linearized equations. If the terms involving explicit division by collision frequencies are ignored, equations (42) can be normalized so that they become

$$\frac{\partial n^+}{\partial \bar{t}} - \frac{\mu^+}{\mu^-}\left(\frac{\partial^2 n^+}{\partial x^2} - \frac{\lambda_{D-}}{\lambda_E}\frac{\partial n^+}{\partial \bar{x}} - n^+\right) - \left(\bar{\nu}_i + \frac{\mu^+}{\mu^-}\right)n^- = 0 \tag{73}$$

$$-n^+ + \frac{\partial n^-}{\partial \bar{t}} - \left[\frac{\partial^2 n^-}{\partial \bar{x}^2} + \frac{\lambda_{D-}}{\lambda_E}\frac{\partial n^-}{\partial \bar{x}} - (1-\bar{\nu}_i)\right]n^- = 0. \tag{74}$$

Here the normalized variables are

$$\begin{aligned} \bar{x} &= x/\lambda_{D-} \\ \bar{t} &= tD^-/\lambda_{D-}^2 \end{aligned} \tag{75}$$

and the following definitions are made

$$\begin{aligned} \bar{\nu}_i &= \nu_i \lambda_{D-}^2/D^- \\ \lambda_E &= T_-/E_o. \end{aligned} \tag{76}$$

Normally, the electron density can be expected to establish itself rapidly in equilibrium with the ion density. In order to determine how rapidly this occurs, assume the ion density in (74) is the excitation for the ion equation and has the form of an impulse located at the spatial origin but constant in time. Let

$$n^+(\bar{x}, \bar{t}) = u_o(\bar{x})\, u_{-1}(\bar{t}).$$

The solution to Eq. 74 in this case is the time integral of the two-dimensional Green's function for the equation.

$$G(\bar{x}, \bar{t}) = \frac{1}{2\lambda_{D-}}\left[\frac{\exp[-\bar{t}(1-\bar{\nu}_i)]}{(\pi\bar{t})^{1/2}}\exp\left[\frac{-\left(\bar{x} + \frac{\lambda_{D-}}{\lambda_E}\bar{t}\right)^2}{4t}\right]\right.$$

$$\left. + \frac{\exp\left(-\frac{\lambda_{D-}}{\lambda_E}\bar{x}\right)}{\left(1+\lambda_{D-}^2/2\lambda_E^2\right)^{1/2}}\exp\left[-\left(1 + \frac{\lambda_{D-}^2}{2\lambda_E^2}\right)^{1/2}\right]|\bar{x}|\right]. \tag{77}$$

It is immediately apparent that the time-dependent part of the problem decays at the rate

$$\tau = \frac{1}{1 - \bar{\nu}_i}.$$

Since the normalized ionization rate is always much less than one, the time constant is about equal to the characteristic time. This is a very small time, usually of the order of 10^{-9} second, which leads to the conclusion that the time-dependent part of the solution can be ignored if the change in the ion density is small in terms of this order of magnitude.

Unless the plasma density is very low, $\lambda_{D-}/\lambda_E \ll 1$ to a good approximation. Therefore, even the spatially dependent part of the solution (77) can be simplified to

$$G(\bar{x}, \bar{t}) \doteq \frac{1}{2\lambda_{D-}} e^{-|x|}. \tag{78}$$

This solution is intuitively correct because it implies that for high plasma densities, where the Debye length is very small, the distribution of the electrons about the positive ion impulse would be very nearly a spatial impulse. The equation for the positive charge density can now be written in the following way.

$$\frac{\partial n^+}{\partial \bar{t}} - \frac{\mu^+}{\mu^-}\left(\frac{\partial^2 n^+}{\partial \bar{x}^2} - \frac{\lambda_{D-}}{\lambda_E}\frac{\partial n^+}{\partial \bar{x}} - n^+\right) = \left(\bar{\nu}_i + \frac{\mu^+}{\mu^-}\right)\int G(\bar{x}-x')\, n^+(x')\, dx'. \tag{79}$$

If the Debye length were zero, the convolution integral would just yield n^+. Two of the terms in the equation would just cancel, and a third could be dropped because $\lambda_{D-} = 0$. The result would be the ambipolar diffusion equation.

If λ_{D-} were large enough to make the approximate Green's function nonimpulsive, and still small enough to allow the approximation $\frac{\lambda_{D-}}{\lambda_E} \ll 1$, then the damping represented by the term $\frac{\mu^+}{\mu^-} n^+$ would no longer be cancelled by the integral contribution. Therefore the instability introduced by the ionization rate is rapidly erased as the Debye length is increased.

In order for Eq. 79 to have solutions that are characteristic of a traveling wave, two conditions must be met. The Debye length must not be too large so that the large damping term is not substantially cancelled; and it must not be too small so that the equations become characteristic of ambipolar diffusion. The similarity between this result and the regimes of instability found in the experiments is apparent.

Another apparent result is that the ionization rate must play an important role in producing the traveling instability. When it is simply held constant, the possible unstable behavior outlined above is the only result. Damping of the solution to Eq. 79 could either be provided by a variable ionization rate, or by inclusion of a frequency or

wavelength-dependent loss term in the kernel $G(\bar{x})$.

5.5 DIFFUSION DAMPING

Diffusion to the walls of the tube can provide a particle loss mechanism for traveling density waves in plasmas, even though it has been shown that this cannot be a simple equilibrium process in the zero-order mode. The excess particles that are created will diffuse to the walls in higher order modes and cause the existence of a finite-loss mechanism. This type of loss would significantly damp wave numbers whose associated phase velocity is small because the diffusion would be in the lower order modes where the radial particle densities are largest. For wave numbers whose associated phase velocity is large, however, diffusion would be in the higher order modes in which the particle current densities, which are proportional to $J_1(x)$ evaluated at the more remote zeros of $J_0(x)$, are much smaller.

A phenomenological loss mechanism should be included in the plane-wave analysis to attempt to bring it more into line with the boundary conditions that exist in the tubes used in the experiments. Our discussion will provide a heuristic basis for assigning the strength of the loss mechanism in a plausible way.

VI. CONCLUSION AND SUGGESTIONS FOR FURTHER RESEARCH

6.1 SUMMARY OF MAJOR RESULTS

The aim at the outset of this investigation was to analyze and clarify the basic processes involved in the propagation of traveling density variations in glow-discharge plasmas in the diffusion range of pressures. In the course of the work, a quasi-stable regime of operation was defined and experimental observations were made in it by the application of current impulses to the electrodes of a discharge tube to obtain traveling small-signal perturbations in the discharge plasma. It is clearly shown in Section III that these waves, induced in an otherwise quiescent plasma, represent a small-signal disturbance and that it should be possible to develop a perturbation analysis of the plasma equations which will lead to a basic understanding of the processes involved in the propagation.

The linearized one-dimensional theory considered in Section IV is an attempt to attain this objective. It leads to the result that an ionization-induced instability can be predicted in glow-discharge plasmas under conditions that are similar to those found in experiments in which the plasma is unstable. A modification of the theory would be necessary, however, to explain completely the linear behavior exhibited by the plasma in the stable regime of operation and, in fact, to establish fully the connection between the theory and the experiments that were performed.

Both the experiments and the theory considered in this report lead to the conclusion that the observed traveling density waves constitute a phenomenon related to ionization, and it is proper to call them ionization waves.

6.2 SUGGESTIONS FOR FURTHER RESEARCH

During the course of this investigation many other areas of research have suggested themselves, and attention to them is clearly necessary if the original objective is to be completely attained. Several important experimental investigations remain to be undertaken. The study of externally excited traveling pulses must be carried farther in several ways. A more efficient method of excitation should be found. The method that was used in this study was impulsive in time but caused the current throughout the tube to change abruptly. This resulted in a poorly launched wave that took several centimeters to settle down to the linear characteristics described in the experiments. A more localized excitation with separate electrodes would be desirable and more efficient.

Tubes of several different diameters should be used to check the relationship between the wavelength of the pulse structure and the critical wavelength predicted by the theory. Also, the lengths of the tubes should be extended to several meters to allow a more precise measurement of the pulse damping.

The spacial structure of the wave packet could also be determined in a manner similar to that described for the nonlinear case in section 2.8. Although the signal levels are small, it would not be impossible to make these measurements with Langmuir probes,

as preliminary measurements carried out during the thesis research showed.

Finally, some method of coupling to the traveling pulse might be attempted with a slow electromagnetic wave, or perhaps with a sound wave separately excited in the neutral gas. Since the group velocity of the pulse can be quite close to the sound velocity in some gases, the coupling between the two might be measureable if the interaction is allowed to extend over a considerable distance.

Extensions and developments that are required for the linearized theory include the further study of the damping mechanisms discussed in Section V and the role of the variable ionization rate in the growth of the instabilities.

APPENDIX A

Alternative Derivation of Ion Sound-Wave Equations

The equations of motion for the plasma will be derived in a manner somewhat different from that of Langmuir and more in keeping with the point of view of transport theory. The method will allow the approximations to be clarified and avoid the necessity of assuming a Boltzmann equilibrium for the electrons in the potential field created by the ions as Langmuir assumed. It will be clear from the derivation that additional requirements are necessary to make the theory generally applicable to the plasma at pressures encountered in glow discharges. Ion-neutral collisions will be discussed in Appendix B, and a rigorous treatment of the glow-discharge problem has been given in Section IV.

First consider the system of equations that represent the expression of conservation of mass, conservation of momentum, and Poisson's equation for the conservation of electric flux. The mass and momentum equations are written separately for ions and electrons.

Conservation of Mass

$$\frac{\partial n^+}{\partial t} + \nabla \cdot \left(n^+ \bar{v}_{d+}\right) = 0 \tag{A-1}$$

$$\frac{\partial n^-}{\partial t} + \nabla \cdot \left(n^- \bar{v}_{d-}\right) = 0. \tag{A-2}$$

Conservation of Momentum

$$\frac{\partial}{\partial t}\left(Mn^+ \bar{v}_{d+}\right) + \nabla\left(n^+ eT_+\right) - n^+ e\bar{E} = 0 \tag{A-3}$$

$$\frac{\partial}{\partial t}\left(mn^- \bar{v}_{d-}\right) + \nabla\left(n^- eT_-\right) + n^- e\bar{E} = 0. \tag{A-4}$$

Poisson's Equation

$$\nabla \cdot \bar{E} = \frac{e}{\epsilon_o}(n^+ - n^-). \tag{A-5}$$

The symbols have the following meanings:

$n^{\pm}$, charged-particle densities

$v_{d\pm}$, charged-particle drift velocities

M, m, ion and electron masses, respectively

$T_{\pm}$, temperatures of the charged particles in volts

e, electronic charge

$\bar{E}$, electric field intensity

ϵ_o, permittivity of free space.

Losses of particles by recombination, attachment, and diffusion toward sinks are not included in the continuity equation. Generation of particles by ionization is also not accounted for, and the only loss of particle density included is that of particle drifts away from some regions of the gas into other regions.

In the momentum equation, the changes in momentum of the particles at any position within the plasma are assumed to be due to gradients in the random energy of the particles and to the electric forces exerted by the local electric fields. It is assumed that no momentum is exchanged between particle species because of binary collisions, nor is any momentum transferred to the neutral gas. Of course, this is quite unrealistic and will be corrected for. But, for the present, only elastic collisions among the individuals of a single species are allowed; and no momentum is lost from the species in that type of encounter.

These five equations may be linearized and reduced to just two equations in two unknowns by the following steps. First, assume that the temperatures of the particles remain constant throughout the plasma. Then the quantity $eT_{\pm}$ may be treated as a constant in the gradient operation on (neT). Next, assume that the product of nE, which makes the momentum equations nonlinear, is linearized by assuming that there is no steady electric field and that the product of the small variation in particle density by that of the electric field will be neglected. Assume also that the zero-order particle densities are the same everywhere and are equal to a constant.

$$n_o^+ = n_o^- = n_o \tag{A-6}$$

Take the divergence of (A-3) and (A-4). Then substitute (A-1), (A-2), and (A-3) in the appropriate places. The results, after division by mass, will be

$$-\frac{\partial^2 n^+}{\partial t^2} + \nabla^2\left[\frac{n^+ eT_+}{M}\right] - \omega_{p+}^2 n^+ + \omega_{p+}^2 n^- = 0 \tag{A-7}$$

$$-\frac{\partial^2 n^-}{\partial t^2} + \nabla^2\left[\frac{n^- eT_-}{m}\right] + \omega_{p-}^2 n^+ - \omega_{p-}^2 n^- = 0, \tag{A-8}$$

where

$$\omega_{p+}^2 = \frac{n_o e^2}{M\epsilon_o}$$

$$\omega_{p-}^2 = \frac{n_o e^2}{m\epsilon_o}. \tag{A-9}$$

The dispersion equation for ion oscillations may be obtained from these two equations by assuming a one-dimensional problem and selecting plane-wave solutions as the prototype solution to be sought. Therefore let the particle densities both vary as follows:

$$n^+(x,t) = N^+ e^{j(\omega t+\beta x)}$$

$$n^-(x,t) = N^- e^{j(\omega t+\beta x)} \tag{A-10}$$

where $N^{\pm}$ are complex amplitudes. The result is

$$\left[\omega^2-\omega_{p+}^2\right] N^+ + \omega_{p+}^2 N^- = 0 \tag{A-11}$$

$$\omega_{p-}^2 N^+ + \left[\omega^2-\frac{eT_-}{M}\beta^2-\omega_{p-}^2\right] N^- = 0, \tag{A-12}$$

where the temperature of the ions has been set equal to zero.

In order for these equations to have a nontrivial solution, the determinant of the coefficients of the complex densities must be zero. That relation is

$$\frac{\omega^4}{\omega_{p-}^2} - \left[1 + \lambda_{D-}^2\beta^2 + \frac{\omega_{p+}^2}{\omega_{p-}^2}\right]\omega^2 + \omega_{p+}^2\lambda_{D-}^2\beta^2 = 0, \tag{A-13}$$

where

$$\lambda_{D-}^2 = \frac{eT_-}{m\omega_{p-}^2} = \frac{\epsilon_o T_-}{n_o e} \tag{A-14}$$

is the electron Debye length.

In this form it is possible to reduce this general result to the dispersion equation for ion sound waves. For small values of ω the biquadratic equation may be represented by its last two terms. With the additional simplification $\omega_{p+} \ll \omega_{p-}$, the result may be written in two explicit forms:

$$\frac{\omega^2}{\omega_{p+}^2} = \frac{\beta^2\lambda_{D-}^2}{1 + \beta^2\lambda_{D-}^2} \tag{A-15}$$

and

$$\lambda_{D-}^2\beta^2 = \frac{\omega^2/\omega_{p+}^2}{1 - \omega^2/\omega_{p+}^2}. \tag{A-16}$$

It is seen from (A-16) that there is propagation of the wave for frequencies below the ion plasma frequency. But the wave is cut off for frequencies above the ion plasma frequency.

When the wavelength that is being propagated is much longer than an electron Debye length, Eq. A-15 reduces to the simple ion sound wave dispersion equation

$$\omega = \omega_{p+}\lambda_{D-}\beta. \tag{A-17}$$

From this relation the so-called ambipolar sound velocity, V_{sa}, may be identified.

$$V_{sa} = \omega_{p+}\lambda_{D-} = \left(\frac{eT_-}{M}\right)^{1/2} . \tag{A-18}$$

Equation A-18 is the relationship that workers attempting to detect ion sound waves generally try to verify.[26]

If, at the point where the temperatures are assumed to be constant (isothermal sound waves), one assumes instead that the propagating disturbance moves so quickly that the process is an adiabatic one, then the only change in (A-18) is the replacement of T_- by γT_-, where γ is the ratio of specific heats. An additional approximation is implied by this substitution. The approximation is introduced at the point where Eqs. A-7 and A-8 are derived. In particular, it is assumed that the electron temperature and density obey the adiabatic relation for an ideal gas:

$$T\, n^{1-\gamma} = \text{constant}. \tag{A-19}$$

As a result, the Laplacian of (nT) is just

$$\nabla^2 nT = \gamma T \nabla^2 n + (\gamma-1)Tn^{-1}(\nabla n)^2. \tag{A-20}$$

It is readily seen that the second term has been dropped in the development under this approximation, and the final result is only true if this term is small compared with the first term. This is certainly the case when small signals are assumed.

The final result of the ion sound-wave theory at wave lengths long compared with the electron Debye length, therefore, is the adiabatic ambipolar sound velocity (Eq. 1)

$$V_{sa} = \left(\frac{\gamma eT_-}{M}\right)^{1/2} .$$

For reference, the principal assumptions made in arriving at this result are as follows:

1. No ionization or recombinations.
2. No collisions between particles of unlike species.
3. Adiabatic process in quasi-static, thermal equilibrium.
4. Ion temperature is zero.
5. Equations are linearized.
6. No zero-order electric field.
7. Zero-order particle densities are equal.
8. $\omega \ll \omega_{p-}$, and $\omega_{p+} \ll \omega_{p-}$, as well as $\lambda_{D-} \ll \lambda$.

APPENDIX B

Collision Damping of Ion Sound Waves

When collisions between the ions and the neutrals and between the electrons and neutral atoms can occur, ion sound waves are appreciably damped at glow-discharge pressures. Consider the modification to the equations of motion of the plasma that result from the inclusion of these collisions. Assume that all of the collisions are elastic; hence, the only effect will be a damping term added to the momentum balance equations. In this case, Eqs. A-3 and A-4 become

$$\frac{\partial}{\partial t}\left(Mn^{+}\bar{v}_{d+}\right) + \nabla\left(n^{+}eT_{+}\right) - n^{+}e\bar{E} = -\nu_{M}M\bar{v}_{d+}n^{+} \tag{B-1}$$

$$\frac{\partial}{\partial t}\left(mn^{-}\bar{v}_{d-}\right) + \nabla\left(n^{-}eT_{-}\right) + n^{-}e\bar{E} = -\nu_{m}m\bar{v}_{d-}n^{-}. \tag{B-2}$$

Here it is assumed that a fraction of the momentum of each particle of the plasma is lost at each collision with a neutral atom. The size of the loss of momentum in the direction of the wave will average approximately one-half for ions at each collision, but will be only approximately (m/M) for electrons because of their extremely small mass. The two quantities ν_M and ν_m are the collision frequencies weighted by the appropriate factors to give the collision frequency for momentum transfer.

These two equations may again be reduced with the aid of Eqs. A-1, A-2, and A-5, which have remained unchanged by the assumed collisions, to the following equations.

$$-\frac{\partial^2 n^{+}}{\partial t^2} + \nabla^2\left[\frac{n^{+}eT_{+}}{M}\right] - \omega_{p+}^2 n^{+} + \omega_{p+}^2 n^{-} = \nu_M \frac{\partial n^{+}}{\partial t} \tag{B-3}$$

$$-\frac{\partial^2 n^{-}}{\partial t^2} + \nabla^2\left[\frac{n^{-}eT_{-}}{m}\right] + \omega_{p-}^2 n^{+} - \omega_{p-}^2 n^{-} = \nu_m \frac{\partial n^{-}}{\partial t}. \tag{B-4}$$

These last two equations result from assumptions and approximations identical with those of Eqs. A-7 and A-8. Again the sinusoidal time and space variation is assumed in a one-dimensional problem, and the equations reduce to

$$\left[\omega^2 - \omega_{p+}^2 - j\omega\nu_m\right]N^{+} + \omega_{p+}^2 N^{-} = 0 \tag{B-5}$$

$$\omega_{p-}^2 N^{-} + \left[\omega^2 - \omega_{p-}^2 - \frac{eT_{-}}{M}\beta^2 - j\omega\nu_m\right]N^{-} = 0. \tag{B-6}$$

The resulting determinantal equation is no longer biquadratic in the exciting frequency. It is a full quartic equation.

$$\omega^4 - j\omega^3[\nu_M+\nu_m] - \left[\omega_{p+}^2 + \omega_{p-}^2 + \frac{eT_-}{M}\beta^2 + \nu_M\nu_m\right]\omega^2$$

$$+ j\omega\left[\nu_m\omega_{p+}^2 + \nu_M\omega_{p-}^2 - \frac{\nu_M eT_-}{m}\beta^2\right] + \omega_{p+}^2\frac{eT_-}{m}\beta^2 = 0. \qquad \text{(B-7)}$$

Under the following assumptions, which are reasonable for a glow-discharge plasma, the dispersion polynomial may be approximated by its last three terms. The assumptions are

$$\begin{aligned} &\omega_{p+} \ll \omega_{p-} \\ &\omega \ll \omega_{p-} \\ &(\omega\nu_M+\omega\nu_m)^{1/2} \ll \omega_{p-} \\ &(\nu_M\nu_m)^{1/2} \ll \omega_{p-} \end{aligned} \qquad \text{(B-8)}$$

and the resulting equations written in a form that shows their analogy to Eqs. A-15 and A-16 are just

$$\frac{\omega^2}{\omega_{p+}^2} = \frac{\lambda_{D-}^2\beta^2}{1+\lambda_{D-}^2\beta^2} + j\frac{\frac{\omega}{\omega_{p+}}\cdot\frac{\nu_M}{\omega_{p+}}}{1+\lambda_{D-}^2\beta^2}$$

$$\beta^2\lambda_{D-}^2 = \frac{\left(\frac{\omega}{\omega_{p+}}\right)^2 - j\frac{\omega}{\omega_{p+}}\cdot\frac{\nu_M}{\omega_{p+}}}{1-\frac{\omega^2}{\omega_{p+}^2} + j\frac{\omega}{\omega_{p+}}\cdot\frac{\nu_M}{\omega_{p+}}}.$$

Koons[24] has arrived at a similar result through the inclusion of collision damping in Langmuir's original derivation.

APPENDIX C

Effect of Viscosity on Sound Propagation at Low Pressures

In order to gain familiarity with some results of the effect of viscosity on sound propagation at low pressures, the attenuation resulting from viscous friction is considered first. If one assumes that the sound wave that is being transmitted and attenuated is a plane wave, the equation of motion is simply the wave equation with a loss term proportional to the added kinematic viscosity.

$$\frac{\partial^2 v}{\partial t^2} = V_s^2 \frac{\partial^2 v}{\partial x^2} + \frac{4}{3}\mu' \frac{\partial^3 v}{\partial x^2 \partial t}, \tag{C-1}$$

where $v(x,t)$ is the velocity of an infinitesimally thin slab of fluid, $\mu' = \mu/\rho_o$ is the fluid kinematic viscosity, and V_s is the speed of sound when the viscous effect is negligible.

Equation C-1 is linear and has the plane monochromatic wave solution:

$$v(x,t) = V_o e^{j\omega t} e^{Gx}.$$

The propagation constant $G(\omega)$ is related to the driving frequency in a manner determined by (C-1). We arrive at this relation by direct substitution of the assumed solution in (C-1) to obtain the dispersion relation

$$G^2 = \frac{\omega^2}{V_s^2\left(1 + j\,\dfrac{4\mu'\omega}{3V_s^2}\right)}.$$

The solution of this equation defines the nature of the propagation at each frequency. To a first approximation it is

$$\pm G = \alpha + j\beta = \frac{2\mu'\omega^2}{3V_s^3} + j\frac{\omega}{V_s} \tag{C-2}$$

when the quantity $\dfrac{4\mu'\omega}{3V_s^2}$ is much less than unity. Since the kinematic viscosity is inversely proportional to pressure, this approximation becomes more exact at high pressures and at low exciting frequencies. At low pressures, the validity criterion must be checked carefully before (C-2) is used.

Next, consider the effect of viscosity in decreasing the velocity of sound because of the proximity of the walls of the containing vessel. In the longitudinal mode of oscillation in a cylindrical pipe, viscous friction acts in such a way as to retard the minute longitudinal vibrations of the gas. The problem can be idealized as follows: Consider an infinite plane wall vibrating in a plane parallel to its surface, say in the y-direction. Let the positive half-space in the x-direction be filled with a viscous fluid. Since the

particles near the wall will have the vibratory motion of the plane imparted to them and in turn will transmit some of their motion to neighboring particles farther from the wall, the body of the fluid will be set into vibratory motion. The motion will be the same for all points at a given distance x_o from the wall and will be directed purely in the y-direction. The results of analyzing this problem may easily be transferred to the case of gas vibrating in a stationary cylindrical vessel. It would be well to look more closely at the details of this problem in order to ascertain what order of magnitude this effect may have in glow-discharge tubes.

The equation governing the motion is

$$\rho \frac{\partial v}{\partial t} = \mu \frac{\partial^2 v}{\partial x^2}, \tag{C-3}$$

where v is the velocity of the fluid in the y-direction. The equation is merely a statement of Newton's second law. The forces acting are just viscous shearing forces. If one assumes that the wall is set into simple harmonic motion at the radian frequency ω, then the solution to (C-3) is

$$v = V_o \exp\left(-\sqrt{\frac{\omega\rho}{2\mu}}\, x\right) \mathrm{Cos}\left(\omega t - \sqrt{\frac{\omega\rho}{2\mu}}\, x\right). \tag{C-4}$$

As we see from this solution, the quantity $l_d = \sqrt{\frac{2\mu'}{\omega}}$ defines a skin depth or penetration depth for the disturbance in the x-direction. The magnitude of l_d compared with the diameter of a cylindrical tube determines whether the velocity of sound within the tube is greatly affected by the viscosity of the fluid, thereby causing a loss of momentum by the wave to the wall.

Rayleigh[31] applied the simple solution of the vibrating, infinite, plane-wall problem to the problem of sound in a cylindrical tube by assuming that the viscous skin depth was small, and the effect of the viscous forces on the sound propagation was only a perturbation of the solution with no viscosity. The result in that case is a reduced sound velocity whose magnitude is given by

$$V_{sV} = V_s\left(1 - \frac{1}{r}\sqrt{\frac{\mu'}{2\omega}}\right), \tag{C-5}$$

where r is the radius of the cylinder. This expression is valid when $\ell d/(2r) \ll 1$.

Acknowledgement

During the period of the author's thesis research, many persons contributed toward overcoming the problems associated with such an undertaking. Principal thanks go to his thesis supervisor, Professor William D. Jackson, for providing the climate in which the work could be carried out, as well as for many helpful discussions concerning details of the work itself.

Professor David R. Whitehouse also gave many hours of helpful discussion and comment concerning the work. The author's more immediate colleagues, Professor John P. Penhune, Professor John W. Poduska, and Mr. Gerald B. Kliman contributed immeasureably to the research by providing daily comment and discussion. Mr. Harry C. Koons helped perform the experiments, and did much of the machine computation that was necessary for the completion of this work.

The use of the facilities of the Research Laboratory of Electronics of the Massachusetts Institute of Technology is gratefully acknowledged. Calculations in connection with this study were performed in part at the Computation Center of the Massachusetts Institute of Technology.

References

1. W. Schottky, "Diffusionstheorie der positiven Saule," Physik. Z. 25, 635 (1924).
2. A. V. Engel and M. Steenbeck, Elektrische Gasentladungen, Vol. I and II (Springer Verlag, Berlin, 1932 and 1934).
3. R. Whiddington, "The Passage of Electricity Through Vacuum Tubes," Engineering (London) 120, 20 (1925).
4. A. Wullner, "Studien uber die Entladungen des Inductionsstrones in nit verdunnten Gasen gefullten Raumen," Jubel band, s. 32 (1874).
5. W. Spottiswood, "On Stratified Discharges – II Observations with a Revolving Mirror," Proc. Roy. Soc. (London) 25, 73 (1876).
6. F. W. Aston and T. Kikuchi, "Moving Striations in Neon and Helium," Proc. Roy. Soc. (London) A98, 50 (1920).
7. T. Kikuchi, "On Moving Striations in a Neon Tube," Proc. Roy. Soc. (London) 19, 257 (1921).
8. J. J. Thomson, "On Striations in the Electric Discharge," Phil. Mag. 18, 441 (1909).
9. A. Bramley, "Striated Discharge in Hydrogen," Phys. Rev. 26, 794 (1925).
10. I. Langmuir and L. Tonks, "Oscillations in Ionized Gases," Phys. Rev. 33, 195 (1929).
11. I. Langmuir and H. M. Mott-Smith, "Theory of Collectors in Gaseous Discharges," Phys. Rev. 28, 727 (1926).
12. G. W. Fox, "Oscillations in the Glow Discharge in Argon," Phys. Rev. 37, 815 (1931).
13. R. H. Sloane and C. M. Minnis, "Moving Striations," Nature 135, 436 (1935).
14. W. Pupp, "Oszillographische Sondenmessungen an Laufenden Schichten der Positiven Saule von Edelgasen," Z. Physik 35, 61 (1935).
15. T. M. Donahue and G. H. Dieke, "Oscillatory Phenomena in D. C. Discharges," Phys. Rev. 81, 248 (1951).
16. A. B. Stewart, "Glow Discharge Resonance," J. Opt. Soc. Am. 45, 651 (1955).
17. A. B. Stewart, "Oscillating Glow Discharge Plasma," J. Appl. Phys. 27, 911 (1956).
18. M. J. Druyvesteyn, "Theory of the Positive Column with Moving Striations," Physica 1, 273 (1934).
19. L. Pekarek, "A Theory of the Successive Production of Moving Striations," Czech. J. Phys. 7, 533 (1957).
20. H. S. Robertson, "Moving Striations in Direct Current Glow Discharges," Phys. Rev. 105, 368 (1957).
21. A. Vlasov and I. Bazarov, "On the Theory of Striations," Soviet Phys. – JETP 20, 1098 (1950).
22. M. Shirokov, "On the Theory of Moving Striae," Dokl. Akad. Nauk SSSR 89, 837 (1953).
23. A. B. Stewart, "Oscillating Glow Discharge Plasma," op. cit., p. 913.
24. H. C. Koons, "Ultrasonic Excitation of Ionic Plasma Oscillations," S. B. Thesis, Department of Physics, M. I. T., Cambridge, Mass., 1963.
25. S. C. Brown, Basic Data of Plasma Physics (The Technology Press of Massachusetts Institute of Technology, Cambridge, Mass., and John Wiley and Sons, Inc., New York, 1959), p. 75.
26. I. Alexeff and R. V. Neidigh, "Observations of Ionic Sound Waves in Plasmas: Their Properties and Applications," Phys. Rev. 129, 516 (1963).
27. J. R. M. Coulter, "Negative Striations," Physica 26, 949 (1960).

28. I. Langmuir and H. M. Mott-Smith, "Studies of Electrical Discharges in Gases at Low Pressure," Gen. Elec. Rev. 27, 449 (1924).

29. J. R. M. Coulter, "Generation of Moving Striations at a Gas Anode," Physica 24, 828 (1958).

30. A. H. Van Gorcum, "Moving Striations in Neon-Gas at the Beginning of the Discharge," Physica 2, 535 (1935).

31. Lord Rayleigh, The Theory of Sound, Vol. I and II (Dover Publications, Inc., New York, 1945; see especially Vol. II, p. 316).

32. M. Greenspan, "Propagation of Sound in Rarefied Helium," J. Acoust. Soc. Am. 22, 568 (1950).

33. Cf. Lord Rayleigh, op. cit., Vol. II, footnote, p. 319.

34. W. P. Allis, "Motions of Ions and Electrons," Technical Report 299, Research Laboratory of Electronics, M. I. T., Cambridge, Mass., 1956; see p. 60.

35. J. M. Anderson, "Electron-Ion Recombination in Low-Temperature Gaseous Plasmas – A Survey of Experimental Work," Report No. 61-RL-2817G, General Electric Research Laboratory, Schenectady, N. Y., 1961.

36. D. R. Whitehouse, Course 6.631 Notes, Fall Term 1961, Massachusetts Institute of Technology; see Eq. 15, p. 5, Chapter 10 (unpublished).

37. P. A. Sturrock, "Kinematics of Growing Waves," Phys. Rev. 112, 1488 (1958).

38. S. C. Brown, op. cit., p. 125.

39. Ibid., p. 135.

Bibliography

The publications listed below are not referred to specifically in the text of this report. The author has not found a complete listing of the literature of this field elsewhere. Together with the cited references, this list should remedy that lack.

E. V. Appleton and D. West, "On Ionic Oscillations in the Striated Glow Discharge," Phil. Mag. 45, 879 (1923).

E. B. Armstrong, K. G. Emeleus, and T. R. Neill, "Low Frequency Disturbances in Gaseous Conductors," Proc. Roy. Irish Acad. A54, 291 (1951).

T. C. Chow, "Oscillations and Traveling Striations in an Argon Discharge Tube," Phys. Rev. 37, 574 (1934).

A. W. Cooper, J. R. Coulter, and K. G. Emeleus, "Simultaneous Occurrence of Moving and Standing Waves in a Positive Column," Nature 181, 1326 (1958).

J. R. M. Coulter, "Negative Sections of Moving Striations," Electronics and Control 9, 41 (1960).

J. R. M. Coulter, N. H. K. Armstrong, and K. G. Emeleus, "Moving Striations and Anode Spots in Neon," Proc. Phys. Soc. (London) 77, 476 (1961).

F. W. Crawford and G. S. Kino, "Oscillations and Noise in Low-Pressure D. C. Discharges," Proc. IRE 49, 1767 (1961).

C. W. Davidson and W. E. Farvis, "Microwave Studies of Pulsed Glow Discharges," Phys. Rev. 127, 1858 (1962).

L. H. Dawson, "Movements of Striae in Discharge Tubes under Varying Pressures," Phys. Rev. 29, 610 (1927).

T. M. Donahue, "Moving Striations in Hydrogen and Deuterium Glow Discharges," Phys. Rev. 82, 571 (1951).

K. G. Emeleus and N. L. Oleson, "Empirical Relations for Moving Striations," Proc. Phys. Soc. (London) 73, 526 (1959).

K. G. Emeleus and N. R. Daly, "Ion Oscillations in a Cathode Potential Minimum," Proc. Phys. Soc. (London) B69, 114 (1956).

K. G. Emeleus, "Oscillations and Fluctuations in Gas Discharges," Nuovo cimento 3, 490 (1956).

V. D. Farris, "Note on Moving Striations," J. Electronics 1, 60 (1955).

K. Foulds, "Moving Striations in Low Pressure Mercury Vapor," J. Electronics and Control 1, 270 (1956).

G. W. Fox, "Oscillations in the Glow Discharge in Neon," Phys. Rev. 35, 1066 (1935).

D. Gabor, "Plasma Oscillations," Brit. J. Appl. Phys. 2, 209 (1951).

H. E. Hartig and C. E. Swanson, "Transverse Acoustic Waves in Rigid Tubes," Phys. Rev. 54, 618 (1938).

M. Klerk, "A Contribution to the Investigation of the Striated Positive Column," Proc. Fourth International Conference on Ionization Phenomena in Gases, Upsala, Sweden, 1959, Vol. IIA, p. 283.

G. Lakatos and J. Bito, "Effect of External Resistance on the Motion of Strata of the Positive Column," Soviet Phys. – JETP 32, 902 (1962).

L. B. Loeb, "The Role of the Cathode in Discharge Instability," Phys. Rev. 76, 255 (1949).

A. A. Luchina, "On Longitudinal Vibrations in a Plasma," Soviet Phys. – JETP 1, 12 (1955).

K. W. Meissner and W. F. Miller, "Influence of Irradiation on the Characteristic of a Glow Discharge in Pure Rare Gases," Phys. Rev. 92, 896 (1953).

N. L. Oleson and C. G. Found, "Running Striations and Multiple Electron Temperatures," J. Appl. Phys. 20, 416 (1949).

N. L. Oleson, "Probe Measurements in an Argon Discharge Containing Running Striations," Phys. Rev. 92, 848 (1953).

N. L. Oleson and A. W. M. Cooper, "Moving Striations," Phys. Rev. 105, 1411 (1957).

L. A. Pardue and J. S. Webb, "Ionic Oscillations in the Glow Discharge," Phys. Rev. 32, 946 (1928).

L. Pekarek, "Theory of Moving Striations," Phys. Rev. 108, 1371 (1957).

A. M. Pilon, "Oscillations in Direct Current Glow Discharges," Phys. Rev. 107, 25 (1957).

A. Rutscher, "The Influence of a Magnetic Field on Moving Striations in Glow Discharges," Naturwiss. 45, 54 (1958).

C. Samson, "Moving Strata in the Positive Column of Rare Gas Arc Discharges," Z. Techn. Physik 6, 281 (1925).

W. Schottky, "Wandstrome und Theorie der positiven Saule," Physik. Z. 25, 342 (1954).

H. L. Steele and P. J. Walsh, "Effect of Moving Striations on the Microwave Conductivity of a Coaxial Discharge," J. Appl. Phys. 25, 1435 (1954).

B. Van Manen, "Laufende Schichten in Neon," Physica 1, 967 (1934).

C. J. D. M. Verhagen, "Impedanzmessungen an Gasentladungsrohren," Physica 8, 361 (1942).

R. Whiddington, "The Discharge of Electricity through Vacuum Tubes," Nature 116, 506 (1925).

H. Yoshimoto, "Moving Striations Due to Space Charge Waves," J. Phys. Soc. Japan 13, 471 (1958).

H. Yoshimoto, "Moving Striations in Arc Discharge," J. Phys. Soc. Japan 13, 734 (1958).